SCUOLA INTERNAZIONALE SUPERIORE DI STUDI AVANZATI

SISSA Digital Library

Towards the entanglement negativity of two disjoint intervals for a one dimensional free fermion

(Article begins on next page)

09 March 2020

Towards entanglement negativity of two disjoint intervals for a one dimensional free fermion

Andrea Coser, Erik Tonni and Pasquale Calabrese

SISSA and INFN, via Bonomea 265, 34136 Trieste, Italy.

Abstract. We study the moments of the partial transpose of the reduced density matrix of two intervals for the free massless Dirac fermion. By means of a direct calculation based on coherent state path integral, we find an analytic form for these moments in terms of the Riemann theta function. We show that the moments of arbitrary order are equal to the same quantities for the compactified boson at the self-dual point. These equalities imply the non trivial result that also the negativity of the free fermion and the self-dual boson are equal.

Contents

1. Introduction

The study of the entanglement content of extended quantum systems became in recent times a subject of extremely large theoretical interest (see e.g. the references in [1] as reviews). While the bipartite entanglement for an extended system in a pure state is a well understood subject and it can be quantified by the so-called entanglement entropy (i.e. the von Neumann entropy of the reduced density matrix of one of the two parts), for a mixed state the quantification of the entanglement is a more subtle issue. The observation that the entanglement in a bipartite mixed state is related to the presence of negative eigenvalues in the partial transpose of the density matrix [2] has led to the introduction of the negativity [3] which subsequently has been shown to be an entanglement monotone [4], i.e. a good entanglement measure from a quantum information point of view.

Although the negativity is a "computable measure of entanglement" [3], its direct and explicit computation in a many body system is very cumbersome. This difficulty can be (at least partially) overcome by a replica approach based on the computation of the even moments of the partially transpose density matrix [5]. This recent approach has been already applied to the study of one-dimensional conformal field theories (CFT) in the ground state [5, 6, 7, 8], in thermal state [9, 10], and in non-equilibrium protocols [10, 11, 12, 13], as well as to topological systems [14, 15, 16]. Focusing on 1D CFTs in the ground state, the negativity is explicitly known only for the simple (but non trivial) geometry of two adjacent intervals embedded in a larger system. For the very important case of the entanglement between two disjoint intervals only the limit of close intervals is explicitly known. For arbitrary distances between the intervals, the main difficulty is to find the analytic continuation of the even-integer moments to $n \to 1$, although these moments are analytically known in a few cases [6, 7] (and indeed numerical interpolation techniques [17] have been exploited to have a numerical prediction for the negativity [18]). These analytical studies have been paralleled by several numerical works such as in Refs. [19, 20, 21, 22, 23, 24, 25].

The goal of this manuscript is to investigate the negativity for the one-dimensional CFT of a free fermionic model. The main result is a close analytical form for the moments of the partial transpose of two disjoint intervals for the massless free Dirac fermion reported in Eq. (55). The explicit form of the moments is exactly the same as for the compactified boson at the self-dual point obtained in Ref. [6].

The manuscript is organised as follows. In Sec. 2 we build the partial transpose of the fermionic density matrix using coherent state path integral. In Sec. 3 we provide the analytical form for the moments of the partial transpose of two disjoint intervals and we analyse it. Finally in Sec. 4 we draw our conclusions and discuss some open problems. In a series of four appendices we report a number of technical details.

2. Partial transpose of the reduced density matrix for the free fermion

In this section we provide a path integral formula for the partial transpose of the density matrix for a free fermionic field theory, after a brief review of the result of Eisler and Zimboras [26] for the partial transpose of the reduced density matrix of two disjoint blocks on the lattice.

2.1. Review of the lattice results

We start from the the tight binding model with Hamiltonian

$$H = \frac{1}{2} \sum_{i=1}^{L} \left[c_i^\dagger c_{i+1} + c_{i+1}^\dagger c_i \right], \tag{1}$$

where periodic boundary conditions are assumed. We only consider the model at half filling $k_F = \pi/2$. Since (1) is quadratic in the fermionic operators, it can be diagonalized

in momentum space. The scaling limit of this model is the massless Dirac fermion which is a CFT with $c = 1$. The local Hilbert space $\mathcal{H}_j$ of a single site is two dimensional and we can choose a basis made by the two vectors corresponding to whether the fermion occurs ($|1\rangle$) or not ($|0\rangle$). In this basis the operators c_j and $c_j^\dagger$ act as the creation and annihilation operators, $c_j |0\rangle = c_j^\dagger |1\rangle = 0$, while $c_j^\dagger |0\rangle = |1\rangle$ and $c_j |1\rangle = |0\rangle$. The tight-binding model can be mapped by a Jordan-Wigner transformation into the XX spin chain

$$H_{XX} = \sum_{j=1}^{L} \left[\sigma_j^x \sigma_{j+1}^x + \sigma_j^y \sigma_{j+1}^y \right]. \tag{2}$$

Although these models are mapped one into the other, since the Jordan-Wigner transformation between them is not local, the entanglement (both entropy and negativity) of two disjoint blocks are not equal, as pointed out already in the literature [27, 28].

We always consider the entire system to be in the ground state $|\Psi\rangle$ with density matrix $\rho = |\Psi\rangle \langle \Psi|$. It is useful to introduce the following Majorana fermions [29]

$$a_j^x = c_j + c_j^\dagger, \qquad a_j^y = \mathrm{i}(c_j - c_j^\dagger), \tag{3}$$

which satisfy the anticommutation relations $\{a_r^\alpha, a_s^\beta\} = 2\delta_{\alpha\beta}\delta_{rs}$. The single site Majorana operators can be also written as

$$a_j^x = \Sigma_j^x, \qquad a_j^y = -\Sigma_j^y, \qquad \mathrm{i}\,a_j^x a_j^y = \Sigma_j^z. \tag{4}$$

The operators Σ_j^α on the single site satisfy the algebra of the Pauli matrices, but at different sites they anticommute and so they are not proper spin operators and should not be confused with the σ_j^α in (2). For each site, we also need to define the following unitary operator

$$U_\alpha^{(k)} = e^{\mathrm{i}\frac{\alpha}{2}\Sigma_j^k} = \cos\left(\alpha/2\right)\mathbb{I} + \mathrm{i}\sin\left(\alpha/2\right)\Sigma_j^k, \tag{5}$$

whose action on the Majorana operators (4) can be obtained from the following relation

$$U_{-\alpha}^{(k)} \Sigma_j^b U_\alpha^{(k)} = \left[\delta_{k,b} + (1 - \delta_{k,b}\cos\alpha)\right]\Sigma_j^b + (\sin\alpha)\varepsilon_{kb\ell}\,\Sigma_j^\ell, \tag{6}$$

where $\varepsilon_{kb\ell}$ is the totally antisymmetric tensor such that $\varepsilon_{xyz} = 1$.

In this manuscript we are interested in a subsystem $A = A_1 \cup A_2$ made by two disjoint blocks of lattice sites. Denoting by $B = B_1 \cup B_2$ the complementary set of sites, which is also made by two disjoint blocks, the reduced density matrix is $\rho_A = \mathrm{Tr}_B |\Psi\rangle \langle \Psi|$. This operator is Gaussian and it can be written as [29]

$$\rho_A = \frac{1}{2^{\ell_1 + \ell_2}} \sum w_{12}\, O_1 O_2, \qquad w_{12} = \langle O_2^\dagger O_1^\dagger \rangle, \tag{7}$$

where O_k (with $k \in \{1, 2\}$) is a generic product of Majorana operators in A_k, namely $O_k = \prod_{j \in A_k} (a_j^x)^{\mu_{[j]}^x} (a_j^y)^{\mu_{[j]}^y}$ with $\mu_{[j]}^\alpha \in \{0, 1\}$. The sum in (7) is performed over all possible combinations of $\mu_{[j]}^\alpha$.

Let us consider the operator O_2 and introduce $\mu_2 = \sum_{j \in A_2} (\mu_{[j]}^x + \mu_{[j]}^y)$ the total number of Majorana operators in O_2 and $\mu_2^y = \sum_{j \in A_2} \mu_{[j]}^y$ the number of a_r^y's in O_2. The

transpose of O_2 (which obviously coincides with the partial transpose with respect to A_2 in this case) is given by

$$O_2^T = (-1)^{\tau(\mu_2)}(-1)^{\mu_2^y} O_2, \tag{8}$$

where

$$\tau(\mu_2) = \begin{cases} 0 & (\mu_2 \bmod 4) \in \{0,1\}, \\ 1 & (\mu_2 \bmod 4) \in \{2,3\}. \end{cases} \tag{9}$$

The factor $(-1)^{\tau(\mu_2)}$ in (8) originates from a rearrangement of the $a^{x,y}$'s operators after the transposition, while the factor $(-1)^{\mu_2^y}$ comes from the fact that $(a_r^y)^T = -a_r^y$ and $(a_r^x)^T = a_r^x$ for the Majorana operators occurring in O_2. This extra factor can be removed by a unitary transformation. Another transposition can be naturally defined, namely

$$O_2^{\widehat{T}} = U_{-\pi}^{(x)} O_2^T U_{\pi}^{(x)} = (-1)^{\tau(\mu_2)} O_2, \tag{10}$$

where the unitary $U_{\pi}^{(x)}$ is now a product of terms like (5) over all the sites and it changes the sign of the a_r^y's leaving the a_r^x's untouched. This is the definition introduced in [26] and we will adopt this convention throughout this manuscript. Thus, let us drop the hat in (10) and denote it simply by O_2^T.

Given a block C of contiguous sites, an important ingredient in our analysis is the following string of Majorana operators

$$P_C = \prod_{j \in C} \mathrm{i}\, a_j^x a_j^y, \tag{11}$$

which satisfies $P_C^{-1} = P_C$.

The partial transpose of ρ_A with respect to A_2 can be written as the following sum of two Gaussian operators [26]

$$\rho_A^{T_2} = \frac{1-\mathrm{i}}{2}\, \tilde{\rho}_A + \frac{1+\mathrm{i}}{2}\, P_{A_2} \tilde{\rho}_A P_{A_2} = \frac{1}{\sqrt{2}} \left(e^{-\mathrm{i}\frac{\pi}{4}} \tilde{\rho}_A + e^{\mathrm{i}\frac{\pi}{4}} P_{A_2} \tilde{\rho}_A P_{A_2} \right), \tag{12}$$

where the construction of $\tilde{\rho}_A$ has been reviewed in App. A and P_{A_2} is the string of Majorana operators (11) along A_2.

The computation of $\mathrm{Tr}(\rho_A^{T_2})^n$ through (12) provides an expression containing 2^n terms given by all the combinations of $\tilde{\rho}_0 \equiv \tilde{\rho}_A$ and $\tilde{\rho}_1 \equiv P_{A_2} \tilde{\rho}_A P_{A_2}$, which can be written as

$$\mathrm{Tr}\big(\rho_A^{T_2}\big)^n = \sum_{p_1,p_2,\dots p_n=0,1} \frac{e^{\mathrm{i}\frac{\pi}{4}\sum_i^n p_i}\, e^{-\mathrm{i}\frac{\pi}{4}\left(n-\sum_i^n p_i\right)}}{2^{n/2}}\, \mathrm{Tr}\left[\prod_{k=1}^{n} \tilde{\rho}_{p_k} \right]. \tag{13}$$

This formula can be further simplified noticing that the various terms in the sum are invariant under the exchange $p_i \to 1 - p_i$. Using this and reorganising the terms in the sum, we can write

$$\mathrm{Tr}(\rho_A^{T_2})^n = \frac{1}{2^{n-1}} \sum_{\boldsymbol{p}} 2^{n/2} \cos\left[\frac{\pi}{4}\left(2\sum_{i=1}^{n-1} p_i - n\right)\right] \mathrm{Tr}\left[\tilde{\rho}_0 \prod_{k=1}^{n-1} \tilde{\rho}_{p_k}\right], \tag{14}$$

where the vector $\boldsymbol{p}$ has $n-1$ components equal to 0 or 1 and therefore the sum contains 2^{n-1} terms.

2.2. Fermionic coherent states for a single site

In this subsection, we briefly review the features of the fermionic coherent states [30] which are needed to build the path integral of ρ_A and $\tilde{\rho}_A$. Here we focus on a single site (indeed, the site index will be dropped in this subsection) and in the next subsection the natural extension to many sites will be considered.

The coherent states for fermions are defined through the Grassmann anticommuting variables. If θ_1 and θ_2 are real Grassmann variables, we have that $\theta_i^2 = 0$ for $i \in \{1, 2\}$ and $\theta_1 \theta_2 = -\theta_2 \theta_1$. Since $\theta^2 = 0$, a function $f(\theta)$ of the real Grassman variable can be written as $f(\theta) = f_0 + f_1 \theta$. Given two real Grassmann variables one can build a complex Grassmann variable ζ as follows

$$\zeta = \frac{1}{\sqrt{2}}(\theta_1 + i\,\theta_2), \qquad \zeta^* = \frac{1}{\sqrt{2}}(\theta_1 - i\,\theta_2). \tag{15}$$

The integration over a complex Grassmann variable acts as a derivation; indeed

$$\int d\zeta^* d\zeta = 0, \quad \int d\zeta^* d\zeta\,\zeta = 0, \quad \int d\zeta^* d\zeta\,\zeta^* = 0, \quad \int d\zeta^* d\zeta\,\zeta\,\zeta^* = 1. \tag{16}$$

The coherent states are defined as follows

$$|\zeta\rangle = |0\rangle - \zeta\,|1\rangle, \qquad \langle\zeta| = \langle 0| + \zeta^*\,\langle 1|. \tag{17}$$

Since ζ commutes with $|0\rangle$ and anticommutes with c, $c^\dagger$ and $|1\rangle$, it is straightforward to check that $c\,|\zeta\rangle = \zeta\,|\zeta\rangle$ and $\langle\zeta|\,c^\dagger = \langle\zeta|\,\zeta^*$. Notice that the coherent states do not provide an orthonormal basis. A completeness relation and a formula for the trace of an operator O read respectively

$$\mathbb{I} = \int d\zeta^* d\zeta\; e^{-\zeta^*\zeta}\,|\zeta\rangle\langle\zeta|, \qquad \mathrm{Tr}\,O = \int d\zeta^* d\zeta\; e^{-\zeta^*\zeta}\,\langle -\zeta|\,O\,|\zeta\rangle. \tag{18}$$

Given the above rules, the matrix elements of the identity and of the operators in (4) on the coherent states (17) can be computed, finding that

$$\langle\zeta|\eta\rangle = 1 + \zeta^*\eta = \langle\eta^*| - \zeta^*\rangle, \tag{19}$$

$$\langle\zeta|a^x|\eta\rangle = \zeta^* + \eta = \langle\eta^*|a^x|\zeta^*\rangle, \tag{20}$$

$$\langle\zeta|a^y|\eta\rangle = -i(\zeta^* - \eta) = -\langle\eta^*|a^y|\zeta^*\rangle, \tag{21}$$

$$\langle\zeta|ia^x a^y|\eta\rangle = 1 - \zeta^*\eta = \langle\eta^*|ia^x a^y| - \zeta^*\rangle, \tag{22}$$

where the second rewriting will be useful in the following subsection. Since $i\,a^x a^y\,|\zeta\rangle = |-\zeta\rangle$, we can bring (20) and (21) in the same form of (19) and (22):

$$\langle\zeta|a^x|\eta\rangle = \langle\eta^*|ia^y| - \zeta^*\rangle = -i\,\langle\eta^*|\,U^{(z)}_{-\pi/2}\,a^x\,U^{(z)}_{\pi/2}\,| - \zeta^*\rangle, \tag{23}$$

$$\langle\zeta|a^y|\eta\rangle = \langle\eta^*|ia^x| - \zeta^*\rangle = \quad i\,\langle\eta^*|\,U^{(z)}_{-\pi/2}\,a^y\,U^{(z)}_{\pi/2}\,| - \zeta^*\rangle. \tag{24}$$

Notice that the insertion of $U^{(z)}_{\pi/2}$ and its hermitian conjugate in (19) and (22) has no effect.

2.3. Partial transpose of the reduced density matrix

The coherent state $|\zeta(x)\rangle$ for a lattice is the tensor product of single site coherent states, with x runnig along the whole system or the corresponding subsystem. In the following we consider a lattice system but the final formulas can be extended to a continuous spatial dimension in a straightforward way by interpreting the discrete sums as integrals and integrations over a discrete set of variables as path integrals.

The density matrix of the whole system in the ground state is $\rho = |\Psi\rangle\langle\Psi|$ and its matrix element between two generic coherent states reads

$$\rho(\zeta(x), \eta(x)) = e^{-\zeta^*\eta}\langle\zeta(x)|\Psi\rangle\langle\Psi|\eta(x)\rangle, \qquad (25)$$

where $\zeta^*\eta = \sum_x \zeta^*(x)\eta(x)$, with x labelling the whole system and $e^{-\zeta^*\eta}$ is the normalization factor (see (19)). To obtain the reduced density matrix in A, one first separates the degrees of freedom in A and the ones in B and then traces over the latter ones. Denoting by $|\zeta_A(x_A)\rangle$ and $|\zeta_B(x_B)\rangle$ the coherent states on A and B respectively, we have that $|\zeta(x)\rangle = |\zeta_A(x_A)\rangle\otimes|\zeta_B(x_B)\rangle$. Adopting the notation $|\zeta(x)\rangle = |\zeta_A(x_A), \zeta_B(x_B)\rangle$, the matrix element of ρ_A is given by

$$\rho_A(\zeta_A(x_A), \eta_A(x_A)) = e^{-\zeta_A^*\eta_A}\int D\chi_B^* D\chi_B \, e^{-\chi_B^*\chi_B}\langle\zeta_A, -\chi_B|\Psi\rangle\langle\Psi|\eta_A, \chi_B\rangle, \qquad (26)$$

where $D\chi_B^* D\chi_B = \prod_{x_B} d\chi_B^*(x_B)\, d\chi_B(x_B)$ and the minus sign comes from the trace over B, according to (18). In the continuum limit, the braket $\langle\Psi|\eta_A, \chi_B\rangle$ is the fermionic path integral on the upper half plane where the boundary conditions $\eta_A(x_A)$ and $\chi_B(x_B)$ are imposed in A and B respectively, just above the real axis. Analogously, $\langle\zeta_A, -\chi_B|\Psi\rangle$ is the path integral on the lower half plane. The trace over B is performed by setting the fields along B equal (but with opposite sign) and summing over all the configurations. The resulting path integral is over the whole plane with two open slits along A_1 and A_2, where the boundary conditions η_A and ζ_A are imposed respectively along the lower and the upper edge of A (left panel of Fig. 1).

Let us consider the partial transpose $\rho_A^{T_2}$ with respect to A_2. In App. A the lattice results of [26] that we need in our analysis are briefly reviewed. Remembering that the partial transposition acts only on operators in A_2, from (7) we can write its matrix elements as follows

$$\langle\zeta(x)|\rho_A^{T_2}|\eta(x)\rangle = \frac{1}{2^{\ell_1+\ell_2}}\sum w_{12}\,\langle\zeta_1(x_1)|O_1|\eta_1(x_1)\rangle\langle\zeta_2(x_2)|O_2^T|\eta_2(x_2)\rangle, \qquad (27)$$

where $x_j \in A_j$, with $j \in \{1, 2\}$.

Focussing on the term corresponding to A_2 in (27), from (10), (19)-(24) one finds

$$\langle\zeta_2(x_2)|O_2^T|\eta_2(x_2)\rangle = (-1)^{\tau(\mu_2)}\,\mathrm{i}^{\mu_2^y-\mu_2^x}\,\langle\eta_2^*(x_2)|\,U_{-\pi/2}^{(z)}\,O_2\,U_{\pi/2}^{(z)}\,|-\zeta_2^*(x_2)\rangle, \qquad (28)$$

where the unitary map $U_{-\pi/2}^{(z)}$ acts on all sites. When the number μ_2 of Majorana operators in A_2 is even, from (9) we have that $(-1)^{\tau(\mu_2)} = \mathrm{i}^{\mu_2}$ and therefore

$$\langle\zeta_2(x_2)|(O_2^T)_{\mathrm{even}}|\eta_2(x_2)\rangle = (-1)^{\mu_2^y}\,\langle\eta_2^*(x_2)|\,U_{-\pi/2}^{(z)}\,(O_2)_{\mathrm{even}}\,U_{\pi/2}^{(z)}\,|-\zeta_2^*(x_2)\rangle \qquad (29)$$

$$= \langle\eta_2^*(x_2)|\,U_{-\pi}^{(y)}\,U_{-\pi/2}^{(z)}\,(O_2)_{\mathrm{even}}\,U_{\pi/2}^{(z)}\,U_{\pi}^{(y)}\,|-\zeta_2^*(x_2)\rangle, \qquad (30)$$
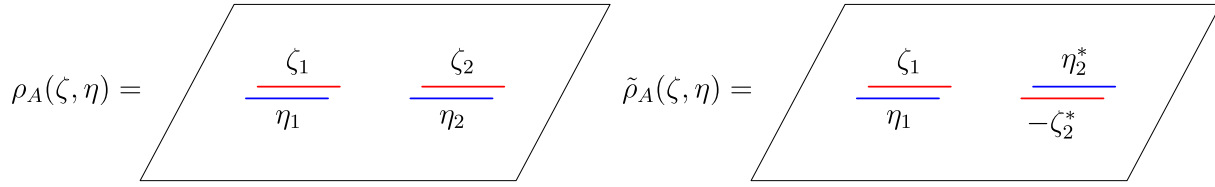
Figure 1. Path integral representation of ρ_A and $\tilde{\rho}_A$ in the coherent state basis.

where in (30) the factor $(-1)^{\mu_2^y}$ has been removed through a second unitary transformation which sends $a_j^x \to -a_j^x$ leaving the a_j^y's unchanged (we recall that $U_{-\pi/2}^{(z)}$ exchanges the a_j^x's with the a_j^y's). The expression (30) suggests us to introduce the following unitary operator acting on A_2

$$V_2 \equiv U_{-\pi}^{(y)} U_{-\pi/2}^{(z)} = \prod_{j \in A_2} \exp\left(-i\frac{\pi}{2}\frac{a_j^x - a_j^y}{\sqrt{2}}\right) = \prod_{j \in A_2} \exp\left[-i\frac{\pi}{2}\left(e^{i\frac{\pi}{4}}c_j^\dagger + e^{-i\frac{\pi}{4}}c_j\right)\right], \quad (31)$$

whose net effect is to send $a_j^x \to -a_j^y$ and $a_j^y \to -a_j^x$, for $j \in A_2$.

In a similar way, we can treat the case of odd μ_2, for which $(-1)^{\tau(\mu_2)} = i^{\mu_2-1}$ (see (9)). Again, from (10), (19)-(24) one gets

$$\langle \zeta_2(x_2)|\left(O_2^T\right)_{\text{odd}}|\eta_2(x_2)\rangle = -i(-1)^{\mu_2^y}\langle \eta_2^*(x_2)|U_{-\pi/2}^{(z)}(O_2)_{\text{odd}}U_{\pi/2}^{(z)}|-\zeta_2^*(x_2)\rangle \quad (32)$$

$$= -i\langle \eta_2^*(x_2)|V_2(O_2)_{\text{odd}}V_2^\dagger|-\zeta_2^*(x_2)\rangle. \quad (33)$$

Introducing the operator $\widetilde{O}_2$ through its matrix elements as follows

$$\langle \zeta_2(x_2)|\widetilde{O}_2|\eta_2(x_2)\rangle = \langle \eta_2^*(x_2)|V_2 O_2 V_2^\dagger|-\zeta_2^*(x_2)\rangle, \quad (34)$$

the expression (27) can be written as follows

$$\langle \zeta(x)|\rho_A^{T_2}|\eta(x)\rangle = \frac{1}{2^{\ell_1+\ell_2}}\left(\sum_{\text{even}} w_{12}\langle \zeta_1(x_1)|O_1|\eta_1(x_1)\rangle\langle \zeta_2(x_2)|\widetilde{O}_2|\eta_2(x_2)\rangle \right. \quad (35)$$

$$\left. -i\sum_{\text{odd}} w_{12}\langle \zeta_1(x_1)|O_1|\eta_1(x_1)\rangle\langle \zeta_2(x_2)|\widetilde{O}_2|\eta_2(x_2)\rangle\right),$$

where in the first (second) sum the terms have an even (odd) number of fermionic operators in A_2 (see App. A). In (35) the structure $\rho_A^{T_2} = \tilde{\rho}_{\text{even}} - i\tilde{\rho}_{\text{odd}}$ (see (68)) can be recognised and this observation leads us to identify the matrix element of $\tilde{\rho}_A$ on the coherent states

$$\langle \zeta(x)|\tilde{\rho}_A|\eta(x)\rangle = \langle \zeta_1(x_1), \eta_2^*(x_2)|V_2 \rho_A V_2^\dagger|\eta_1(x_1), -\zeta_2^*(x_2)\rangle, \quad (36)$$

and analogously

$$\langle \zeta(x)|P_{A_2}\tilde{\rho}_A P_{A_2}|\eta(x)\rangle = \langle \zeta_1(x_1), -\eta_2^*(x_2)|V_2 \rho_A V_2^\dagger|\eta_1(x_1), \zeta_2^*(x_2)\rangle, \quad (37)$$

where from (22) we can read that the action of P_{A_2} is to change the sign of ζ_2. A graphical representation of this path integral representation for $\tilde{\rho}_A$ is given in the right

panel of Fig. 1. Hence, the final expression for the the partial transpose in the coherent state basis can be written exactly like the lattice counterpart i.e.

$$\rho_A^{T_2}(\zeta,\eta) = \frac{1}{\sqrt{2}} \left[e^{-i\frac{\pi}{4}} \tilde{\rho}_A(\zeta_1,\zeta_2;\eta_1,\eta_2) + e^{i\frac{\pi}{4}} \tilde{\rho}_A(\zeta_1,-\zeta_2;\eta_1,-\eta_2) \right], \qquad (38)$$

where the notation is such that $\eta_i,\zeta_i \in A_i$. This explicit form of the partial transpose in the coherent state basis is the final and main result of this section.

In App. B we employ the formalism of this section to check the identity $\mathrm{Tr}(\rho_A^{T_2})^2 = \mathrm{Tr}\rho_A^2$ (which holds for any quantum system [5, 6]) for the free fermion.

3. Traces of the partial transpose for the free fermion

In this section we consider the moments $\mathrm{Tr}(\rho_A^{T_2})^n$ for the free fermion. After summarising some needed CFT results for the moments of ρ_A (Sec. 3.1), using the path integral approach of the previous section, we derive the analytic formula for $\mathrm{Tr}(\rho_A^{T_2})^n$ given by (55) which is the main result of this manuscript. In Sec. 3.3 we show that the moments for the free fermion are equal to the ones for the compact boson at the self-dual radius. Finally, in Sec. 3.4 we give some numerical checks of our results.

3.1. Some CFT results for $\mathrm{Tr}\rho_A^n$

For the case of a single interval of length ℓ embedded in a CFT on the infinite line, the moments of the reduced density matrix can be written as [31, 32, 33]

$$\mathrm{Tr}\rho_A^n = c_n \left(\frac{\ell}{a} \right)^{-c(n-1/n)/6}, \qquad (39)$$

where c is the central charge and a the inverse of an ultraviolet cutoff (e.g. the lattice spacing). The prefactors c_n are non universal constants (that however satisfy universal relations [34]). The simple universal dependence on the central charge can be understood because $\mathrm{Tr}\rho_A^n$ is the partition function on a surface of genus zero that can be mapped to the complex plane [32]. Eq. (39) can be interpreted as the two-point function of some twist operators acting at the endpoints of the interval u and v [32, 35], i.e. $\mathrm{Tr}\rho_A^n = \langle \mathcal{T}_n(u)\bar{\mathcal{T}}_n(v) \rangle$. The twist fields $\mathcal{T}_n$ behave like primary operators with scaling dimension

$$\Delta_n = \frac{c}{12} \left(n - \frac{1}{n} \right). \qquad (40)$$

The knowledge of the moments $\mathrm{Tr}\rho_A^n$ give access to the full spectrum of the reduced density matrix [36]. While c_n is not universal, its value for the tight-binding model at half-filling is known exactly and it is given by [37]

$$c_n = 2^{-\frac{1}{6}\left(n-\frac{1}{n}\right)} \exp\left\{ i n \int_{-\infty}^{\infty} dz \log \left(\frac{\Gamma\left(\frac{1}{2}+iz\right)}{\Gamma\left(\frac{1}{2}-iz\right)} \right) \left[\tanh(\pi z) - \tanh(\pi n z) \right] \right\}. \qquad (41)$$

For the case of two disjoint intervals $A = A_1 \cup A_2 = [u_1, v_1] \cup [u_2, v_2]$, by global conformal invariance, in the thermodynamic limit, $\mathrm{Tr}\rho_A^n$ can be written as (dropping hereafter the dependence on the UV cutoff a)

$$\mathrm{Tr}\rho_A^n = c_n^2 \left(\frac{|u_1 - u_2||v_1 - v_2|}{|u_1 - v_1||u_2 - v_2||u_1 - v_2||u_2 - v_1|} \right)^{2\Delta_n} \mathcal{F}_n(x), \tag{42}$$

where x is the four-point ratio (for real u_j and v_j, x is real)

$$x = \frac{(u_1 - v_1)(u_2 - v_2)}{(u_1 - u_2)(v_1 - v_2)} \in (0, 1). \tag{43}$$

The function $\mathcal{F}_n(x)$ is a universal function (after being normalized such that $\mathcal{F}_n(0) = 1$) that encodes all the information about the operator spectrum of the CFT while c_n is the same non-universal constant appearing in (39). The function $\mathcal{F}_n$ has been studied in several papers [38, 39, 40, 41, 42, 43, 44, 45, 46, 28, 47, 48, 49, 50] (see [51, 44, 52] for the holographic viewpoint and [53] for higher dimensional conformal field theories). In the case of two disjoint intervals, $\mathrm{Tr}\rho_A^n$ is the partition function on a surface of genus $n - 1$ which cannot be mapped to the complex plane. This surface is usually called $\mathcal{R}_n$.

One of the most important examples of exactly known $\mathcal{F}_n(x)$ is the free boson compactified on a circle of radius r_{circle}. In this case, the function $\mathcal{F}_n(x)$ (parametrized in terms of $\eta = 2r_{\mathrm{circle}}^2$) is [38]

$$\mathcal{F}_n(x) = \frac{\Theta(\mathbf{0}|\eta\tau)\,\Theta(\mathbf{0}|\tau/\eta)}{[\Theta(\mathbf{0}|\tau)]^2}, \tag{44}$$

where τ is an $(n-1) \times (n-1)$ matrix (called period matrix) with elements [38]

$$\tau_{i,j} = \mathrm{i}\frac{2}{n}\sum_{k=1}^{n-1} \sin(\pi k/n) \frac{{}_2F_1(k/n, 1 - k/n; 1; 1 - x)}{{}_2F_1(k/n, 1 - k/n; 1; x)} \cos[2\pi(k/n)(i - j)]. \tag{45}$$

We remark that, since $x \in (0, 1)$, the period matrix $\tau(x)$ is purely imaginary. Θ is the Riemann theta function [54, 55]

$$\Theta(\mathbf{z}|M) \equiv \sum_{\mathbf{m} \in \mathbb{Z}^{n-1}} e^{\mathrm{i}\pi\,\mathbf{m}^{\mathrm{t}}\cdot M\cdot\mathbf{m} + 2\pi\mathrm{i}\,\mathbf{m}^{\mathrm{t}}\cdot\mathbf{z}}, \tag{46}$$

which is a function of the $(n-1)$ dimensional complex vector $\mathbf{z}$ and of the $(n-1)\times(n-1)$ matrix M which must be symmetric and with positive imaginary part.

For the critical Ising model, the scaling function $\mathcal{F}_n(x)$ is also known [39]

$$\mathcal{F}_n(x) = \frac{1}{2^{n-1}\,\Theta(\mathbf{0}|\tau)} \sum_{\boldsymbol{\varepsilon},\boldsymbol{\delta}} \left| \Theta\begin{bmatrix}\boldsymbol{\varepsilon}\\\boldsymbol{\delta}\end{bmatrix}(\mathbf{0}|\tau) \right|, \tag{47}$$

where the period matrix τ is the same as in Eq. (45). In this case Θ is the Riemann theta function with characteristic defined as [54, 55]

$$\Theta[\mathbf{e}](\mathbf{z}|M) \equiv \sum_{\mathbf{m} \in \mathbb{Z}^{n-1}} e^{\mathrm{i}\pi(\mathbf{m}+\boldsymbol{\varepsilon})^{\mathrm{t}}\cdot M\cdot(\mathbf{m}+\boldsymbol{\varepsilon}) + 2\pi\mathrm{i}\,(\mathbf{m}+\boldsymbol{\varepsilon})^{\mathrm{t}}\cdot(\mathbf{z}+\boldsymbol{\delta})}, \qquad \mathbf{e} \equiv \begin{pmatrix}\boldsymbol{\varepsilon}\\\boldsymbol{\delta}\end{pmatrix}, \tag{48}$$
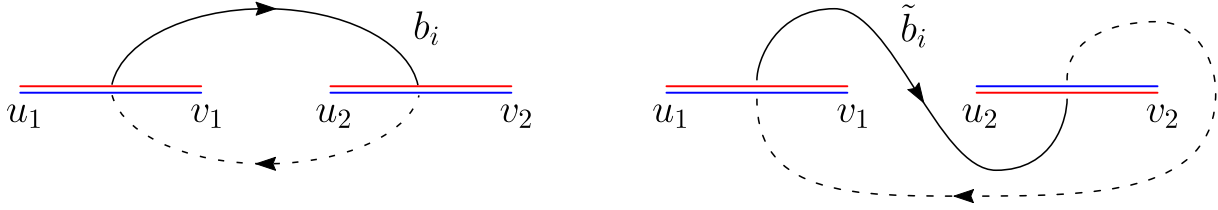
Figure 2. Cycles of type b for $\mathcal{R}_n$ (left) and $\widetilde{\mathcal{R}}_n$ (right). The solid line represents the part of the cycle belonging to the i-th sheet, while the dashed curve is the remaining part of the cycle, which lies in the $(i+1)$-th sheet. As for the cycles of type a, which are the same for $\mathcal{R}_n$ and $\widetilde{\mathcal{R}}_n$, we refer to Fig. 8 of [46].

where $\boldsymbol{z}$ and M are analogous to the ones in (46), and $\boldsymbol{\varepsilon}, \boldsymbol{\delta}$ are vector with entries 0 and $1/2$. The sum in $(\boldsymbol{\varepsilon}, \boldsymbol{\delta})$ in (47) is intended over all the 2^{n-1} vectors $\boldsymbol{\varepsilon}$ and $\boldsymbol{\delta}$ with these entries. The parity of (48) as function of $\boldsymbol{z}$ is given by the parity of the characteristic, which is the parity of the integer number $4\boldsymbol{\varepsilon} \cdot \boldsymbol{\delta}$. There are $2^{2(n-1)}$ characteristics: $2^{n-2}(2^{n-1}+1)$ are even and $2^{n-2}(2^{n-1}-1)$ are odd. In our following analysis only the trivial vector $\boldsymbol{z} = \boldsymbol{0}$ occurs and therefore we will adopt the shortcut notation: $\Theta[\boldsymbol{e}](M) \equiv \Theta[\boldsymbol{e}](\boldsymbol{0}|M)$ and $\Theta(M) \equiv \Theta(\boldsymbol{0}|M)$ when the characteristic is vanishing.

In the computation of the partition function on higher genus Riemann surfaces, one has to properly choose a canonical homology basis (i.e. a set of $2(n-1)$ closed oriented curves on the surface, the a and b cycles, which satisfy some specific intersection rules) and a set of $n-1$ holomorphic differentials. By integrating such differentials along the b cycles one gets the period matrix of the Riemann surface. For a genus g Riemann surface, the period matrix is a $g \times g$ complex symmetric matrix with positive definite imaginary part [56, 57]. We refer the reader to [46] for a detailed analysis about the canonical homology basis for $\mathcal{R}_n$. In particular, the canonical homology basis $\{a_r, b_r \,;\, 1 \leqslant r \leqslant n-1\}$ corresponding to (45) has been discussed in Sec. 4 of [46] and we will adopt it throughout this manuscript. In the left panel of Fig. 2 we show the j-th b cycle, which belongs to the j-th sheet and to the $(j+1)$-th sheet. Instead, the construction of a_j (which intersects b_j only once) is more involved and therefore we refer the interested reader to Fig. 8 of [46].

The Riemann theta function with characteristic (48) occurs in the computation of fermionic models on higher genus Riemann surfaces [56, 57]. The characteristic $\boldsymbol{e}$ specifies the set of boundary conditions along the a and b cycles of the canonical homology basis and this provides the so called *spin structures* of the model. The vector $\boldsymbol{\varepsilon}$ is determined by the boundary conditions along the a cycles ($\varepsilon_k = 0$ for antiperiodic b.c. around a_k and $\varepsilon_k = 1/2$ for periodic b.c.), while $\boldsymbol{\delta}$ is provided by the boundary conditions along the b cycles ($\delta_k = 0$ for antiperiodic b.c. around b_k and $\delta_k = 1/2$ for periodic b.c.).

3.2. Moments of the partial transpose for the free fermionic field theory

We are finally ready to derive the moments of the partial transpose $\mathrm{Tr}(\rho_A^{T_2})^n$. The path integral for $\rho_A^{T_2}$ is given by (38) which is a sum of two different operators. The moments

are then given by the sum of 2^n terms that come from the expansion of the binomial. Actually, since there is a double degeneration of these terms, the sum is only on 2^{n-1} terms. Introducing, in analogy with the lattice computation, the notation $\tilde{\rho}_0(\zeta, \eta) = \tilde{\rho}_A(\zeta, \eta)$ and $\tilde{\rho}_1(\zeta, \eta) = \tilde{\rho}_A(\zeta_1, -\zeta_2; \eta_1, -\eta_2) = P_{A_2}\tilde{\rho}_A P_{A_2}$, the 2^{n-1} terms in the sum for the moment of order n can be written as

$$\int \prod_{k=1}^{n} D\chi_k^* D\chi_k \, \tilde{\rho}_0(-\chi_n, \chi_1) \prod_{k=1}^{n-1} \tilde{\rho}_{p_k}(\chi_k, \chi_{k+1}), \qquad (49)$$

with $p_i = 0, 1$. Each of these 2^{n-1} terms is a partition function of a free fermion on a Riemann surface of genus $n-1$ in which antiperiodic or periodic boundary condition are imposed along the basis cycles.

At this point, before deriving the final result, we should discuss the Riemann surface $\widetilde{\mathcal{R}}_n$ on which these partition functions are defined. The surface $\widetilde{\mathcal{R}}_n$ is defined by the density matrix $\tilde{\rho}_A$ and has genus $n-1$ [5, 6], but it is different from the one defining $\text{Tr}\rho_A^n$ (denoted in the previous section as $\mathcal{R}_n$). Only for $n = 2$ they are the same torus (their moduli are related by a modular transformation), but for $n > 2$ they are different. The properties of this Riemann surface are discussed in details in App. C. The period matrix $\tilde{\tau}(x)$ of $\widetilde{\mathcal{R}}_n$ for $x \in (0, 1)$ is given by [6]

$$\tilde{\tau}(x) = \tau\big(x/(x-1)\big) = \mathcal{R} + i\mathcal{I}, \qquad \mathcal{R} = \frac{1}{2}\mathcal{Q}, \qquad (50)$$

where the elements of τ have been defined in (45) and the real and imaginary parts of $\tilde{\tau}(x)$ are $\mathcal{R}$ and $\mathcal{I}$ respectively. Here it is important to observe that $\mathcal{Q}$ is a very simple symmetric integer matrix: it has 2 along the principal diagonal, -1 along the secondary diagonals and 0 for the remaining elements. In App. C.1 we report the detailed derivation of this result. As for the cycles of $\widetilde{\mathcal{R}}_n$ providing the canonical homology basis $\{\tilde{a}_r, \tilde{b}_r \, ; \, 1 \leqslant r \leqslant n-1\}$ which gives the period matrix (50), we find that $\tilde{a}_r$ is the same as a_r (we remind that $\widetilde{\mathcal{R}}_n$ and $\mathcal{R}_n$ differ only for the way to join the sheets along A_2), while the generic cycle $\tilde{b}_r$ is obtained by deforming the cycle b_r as shown in Fig. 2.

An important ingredient at this point is the operator P_{A_2}. For an arbitrary interval C we can write

$$P_C = (-1)^{\int_C dx \, \bar{\psi}(x)\psi(x)} \equiv (-1)^{F_C}. \qquad (51)$$

where F_C is the fermionic number operator in the interval C which was already introduced long ago [58]. This operator is located along the interval C and it changes the fermionic boundary conditions (from antiperiodic to periodic or viceversa) on a cycle whenever it crosses the curve C. In (38) for $\rho_A^{T_2}$, we have that P_{A_2} occurs both before and after $\tilde{\rho}_A$. This corresponds to the insertion of the operators $(-1)^{F_{A_2}}$ above and below the cut along A_2.

Each term (49) is a partition function on $\widetilde{\mathcal{R}}_n$ with some specific boundary conditions along the a and b cycles and it can be expressed in terms of Riemann theta functions.

Explicitly, we have

$$\mathrm{Tr}\left[\tilde{\rho}_0 \prod_{k=1}^{n-1} \tilde{\rho}_{p_k}\right] = c_n^2 \left(\frac{1-x}{\ell_1 \ell_2}\right)^{2\Delta_n} \left|\frac{\Theta[\boldsymbol{e}](\tilde{\tau}(x))}{\Theta(\tilde{\tau}(x))}\right|^2, \qquad \boldsymbol{e} = \begin{pmatrix} \boldsymbol{0} \\ \boldsymbol{\delta} \end{pmatrix}, \tag{52}$$

where $\boldsymbol{0}$ is the vector made by $n-1$ zeros. In this formula we have still to fix the vector $\boldsymbol{\delta}$ in terms of $\boldsymbol{p}$, which is done as follows. Eq. (49) is evaluated on the n-sheeted Riemann surface $\widetilde{\mathcal{R}}_n$ where the i-th sheet is associated to the $\tilde{\rho}_{p_i}$. On the sheets associated to $\tilde{\rho}_1$, two operators $(-1)^{F_{A_2}}$ must be placed above and below A_2. Then, the spin structure $\boldsymbol{e}$ can be read off by counting how many times the cycles of the basis cross the curves A_2. Since the cycles $\tilde{a}_i$ do not intersect A_2 at all, we have that $\boldsymbol{\varepsilon} = \boldsymbol{0}$, i.e. the boundary conditions for the fermion along all the cycles $\tilde{a}_r$ are antiperiodic. Instead, for $\tilde{b}_r$ this analysis is non trivial because it intersects A_2 on the r-th sheet and on the $(r+1)$-th sheet, as one can see from the right panel of Fig. 2. If $\tilde{b}_r$ crosses these curves an even number of times, then $\delta_r = 0$, otherwise $\delta_r = 1/2$. It is not difficult to conclude that

$$2\delta_i = (p_i + p_{i+1}) \bmod 2, \tag{53}$$

whose inverse reads

$$p_i = \left(\sum_{j=i}^{n-1} 2\delta_j\right) \bmod 2 = \frac{1-(-1)^{2\sum_{j=i}^{n-1}\delta_j}}{2}. \tag{54}$$

The simplest example of (52) is the term $\mathrm{Tr}\tilde{\rho}_0^n$ (namely $\boldsymbol{p} = \boldsymbol{0}$). This spin structure has antiperiodic boundary conditions along all the cycles, i.e. $\boldsymbol{\varepsilon} = \boldsymbol{\delta} = \boldsymbol{0}$. For this term $\widetilde{\Omega}_n[\boldsymbol{e}]^2 = 1$.

Thus, $\mathrm{Tr}\left(\rho_A^{T_2}\right)^n$ can be written as a sum over all the allowed spin structures:

$$\mathrm{Tr}\left(\rho_A^{T_2}\right)^n = c_n^2 \left(\frac{1-x}{\ell_1 \ell_2}\right)^{2\Delta_n} \frac{1}{2^{n-1}} \sum_{\boldsymbol{\delta}} r_n(\boldsymbol{\delta}) \left|\frac{\Theta[\boldsymbol{e}](\tilde{\tau})}{\Theta(\tilde{\tau})}\right|^2, \qquad \boldsymbol{e} = \begin{pmatrix} \boldsymbol{0} \\ \boldsymbol{\delta} \end{pmatrix}. \tag{55}$$

The coefficient $r_n(\boldsymbol{\delta})$ is

$$r_n(\boldsymbol{\delta}) = 2^{n/2} \cos\left[\frac{\pi}{4}\left(1 + \sum_{i=1}^{n-1}(-1)^{2\sum_{j=i}^{n-1}\delta_j}\right)\right]. \tag{56}$$

It can be seen that $r_n(\boldsymbol{\delta}) \in \{-2^{n/2}, 0, 2^{n/2}\}$ for even n and $r_n(\boldsymbol{\delta}) \in \{-2^{(n-1)/2}, 2^{(n-1)/2}\}$ for odd n.

The analytic expression given by (55) and (56) is the main result of this manuscript. When the size of the intervals is very small with respect to their distance ($\ell_1, \ell_2 \ll d$. i.e. $x \ll 1$), it is possible to expand (55) in powers of x, as shown in App. C.2 where we find the first non trivial term of this expansion.

There is also a very interesting by-product of our analysis which is given by (52) providing a very deep technical insight. Indeed Eq. (52) shows also that *each of the 2^{n-1} terms in the sum over $\boldsymbol{p}$ in (14) has a well defined continuum limit* which is the partition function of the free fermion on $\widetilde{\mathcal{R}}_n$ with a particular assignment of fermionic boundary conditions, i.e. always antiperiodic along all the a cycles, while the b.c. along the b cycles are specified by $\boldsymbol{\delta}$ (we recall, antiperiodic for $\delta_i = 0$ and periodic otherwise).

3.2.1. Dihedral symmetry. The Riemann surfaces $\mathcal{R}_n$ and $\widetilde{\mathcal{R}}_n$ enjoy a dihedral symmetry $\mathbb{Z}_n \times \mathbb{Z}_2$, as already noticed in [45]. The symmetry $\mathbb{Z}_n$ comes from the invariance under cyclic permutation of the n sheets and the symmetry $\mathbb{Z}_2$ corresponds to take the sheets in the reversed order and to reflect all of them with respect to the real axis. The former symmetry comes from the fact that $\mathcal{R}_n$ and $\widetilde{\mathcal{R}}_n$ are obtained through the replica construction and the latter one occurs because the endpoints of the intervals are on the real axis. Indeed, the complex equations (73) and (74), which define the Riemann surfaces $\mathcal{R}_n$ and $\widetilde{\mathcal{R}}_n$, are invariant under complex conjugation.

In [45, 46] the symplectic matrices which implement the dihedral symmetry of $\mathcal{R}_n$ have been written explicitly and in App. C.3 this analysis has been extended to $\widetilde{\mathcal{R}}_n$ as well (the symmetry $\mathbb{Z}_2$ is different in the two cases). These transformations act on the period matrix and reshuffle the characteristics, but the functions and $\widetilde{\Omega}_n[\boldsymbol{e}]$ in (63) remain invariant. Moreover, both the transformations associated to the dihedral symmetry leave the coefficient $r_n(\boldsymbol{\delta})$ in (56) invariant. Thus, the terms in the sum (55) whose characteristics are related by one of these modular transformations are equal and the sum can be written in a simpler form by choosing a representative term for each equivalence class, whose coefficient is given by (56) multiplied by the number of terms of the equivalence class.

Exploiting these symmetries, one can write the explicit expressions given in Sec. 6.3 of [59] for $2 \leqslant n \leqslant 5$. Beside the goal of having more compact analytic expressions, the dihedral symmetry is very helpful also from the numerical point of view because it allows to reduce the exponentially large (in n) number of terms in (55).

Looking at Eq. (13) on the lattice, the $\mathbb{Z}_n$ symmetry corresponds to the cyclic permutation of the n factors within each trace. Instead, the $\mathbb{Z}_2$ symmetry comes from the fact that $\tilde{\rho}_0$ and $\tilde{\rho}_1$ are not separately hermitian but the hermitian conjugation exchange them, so that $\rho_A^{T_2}$ is hermitian. However, as already noticed, such exchange leaves any term of the sum unchanged.

3.3. Self-dual boson

In this subsection we show that the expression (55) for $\text{Tr}\left(\rho_A^{T_2}\right)^n$ of the Dirac free fermion is equal to the one for the compactified boson at its self-dual radius.

The analytic formula for $\text{Tr}\left(\rho_A^{T_2}\right)^n$ of the compactified boson for a generic value of the compactification radius has been derived in [6] by studying the partition function of the model on the Riemann surface $\widetilde{\mathcal{R}}_n$. At the self-dual radius, it becomes (see Eq. (146) of [6] for $\eta = 1$)

$$\text{Tr}\left(\rho_A^{T_2}\right)^n = c_n^2 \left(\frac{1-x}{\ell_1 \ell_2}\right)^{2\Delta_n} \frac{\Theta(T)}{|\Theta(\tilde{\tau})|^2}, \qquad T = \begin{pmatrix} i\mathcal{I} & \mathcal{R} \\ \mathcal{R} & i\mathcal{I} \end{pmatrix}, \tag{57}$$

where the matrices occurring in this expression have been defined in (50). The Riemann

theta function $\Theta(T)$ in the numerator can be written as follows

$$\Theta\begin{pmatrix} i\mathcal{I} & \mathcal{R} \\ \mathcal{R} & i\mathcal{I} \end{pmatrix} = \sum_{\boldsymbol{\varepsilon}} \left| \Theta\begin{bmatrix} \boldsymbol{\varepsilon} \\ \mathbf{0} \end{bmatrix}(2\tilde{\tau}) \right|^2 = \sum_{\boldsymbol{\varepsilon}} e^{2\pi i \boldsymbol{\varepsilon}\cdot\mathcal{Q}\cdot\boldsymbol{\varepsilon}} \, \Theta\begin{bmatrix} \boldsymbol{\varepsilon} \\ \mathbf{0} \end{bmatrix}(2\tilde{\tau})^2, \qquad (58)$$

where in the first step we have used (3.6b) of [57] and in the second one $-2\tilde{\tau}^* = 2\tilde{\tau} - 2\mathcal{Q}$. Then, by specialising the addition formula reported in [55] (pag. 4) to our case, we find

$$\Theta\begin{pmatrix} i\mathcal{I} & \mathcal{R} \\ \mathcal{R} & i\mathcal{I} \end{pmatrix} = \frac{1}{2^{n-1}} \sum_{\boldsymbol{\varepsilon},\boldsymbol{\delta}} (-1)^{4\boldsymbol{\varepsilon}\cdot\boldsymbol{\delta}} \, e^{2\pi i \boldsymbol{\varepsilon}\cdot\mathcal{Q}\cdot\boldsymbol{\varepsilon}} \, \Theta\begin{bmatrix} \mathbf{0} \\ \boldsymbol{\delta} \end{bmatrix}(\tilde{\tau})^2 = \frac{1}{2^{n-1}} \sum_{\boldsymbol{\delta}} m_n(\boldsymbol{\delta}) \, \Theta\begin{bmatrix} \mathbf{0} \\ \boldsymbol{\delta} \end{bmatrix}(\tilde{\tau})^2, \quad (59)$$

where

$$m_n(\boldsymbol{\delta}) = \sum_{\boldsymbol{\varepsilon}} (-1)^{4\boldsymbol{\varepsilon}\cdot\boldsymbol{\delta}} \, e^{2\pi i \boldsymbol{\varepsilon}\cdot\mathcal{Q}\cdot\boldsymbol{\varepsilon}} = \sum_{\boldsymbol{\varepsilon}} e^{4i\pi\left(\boldsymbol{\varepsilon}\cdot\frac{\mathcal{Q}}{2}\cdot\boldsymbol{\varepsilon}+\boldsymbol{\varepsilon}\cdot\boldsymbol{\delta}\right)}. \qquad (60)$$

In App. D we show that $m_n(\boldsymbol{\delta})$ can be written as the partition function of a classical Ising spin system, where $\boldsymbol{\varepsilon}$ play the role of the spin variables and the $\boldsymbol{\delta}$ are the local magnetic fields. In the same appendix we also employ standard transfer matrix techniques to prove that $m_n(\boldsymbol{\delta}) = r_n(\boldsymbol{\delta})$ (see (56) and (60)).

3.4. Numerical checks

In [59] we have already shown that $\mathrm{Tr}(\rho_A^{T_2})^n$ for $n = 3, 4, 5$ converges in the continuum limit to the CFT predictions (55). In this paper we have given a set of more stringent relations (52) between each term in the sum for $\mathrm{Tr}(\rho_A^{T_2})^n$ appearing both in CFT and on the lattice. The goal of this subsection is to provide explicit numerical evidence of this term-by-term correspondence for $n = 2, 3, 4$.

In order to evaluate numerically the traces of product of these matrices, we employ the techniques first developed in [60] for $\mathrm{Tr}\rho_A^n$ and recently used to compute $\mathrm{Tr}(\rho_A^{T_2})^n$ in [59]. Indeed, being the tight-binding Hamiltonian (1) quadratic in the fermionic operators, the ground state reduced density matrix ρ_A is Gaussian. Moreover, $\tilde{\rho}_A$ in (12) is Gaussian as well and, since the string operator P_C can be written as the exponential of a quadratic operator, the density matrix $P_{A_2}\tilde{\rho}_A P_{A_2}$ is also Gaussian. Nevertheless, the sum of these two matrices in (12) is not Gaussian (this is indeed the main difficulty compared to bosonic models in which the partial transpose is itself Gaussian [61, 62, 63, 64]). By exploiting the fact that for Gaussian states all the information of the system is encoded in the correlation matrices, the computations can be performed in a polynomial time in terms of the total size of the subsystem. In particular, in our case the correlation matrices of $\tilde{\rho}_A$ and $P_{A_2}\tilde{\rho}_A P_{A_2}$ can be obtained from the one of ρ_A, as described in [26, 59].

The lattice computations have been performed in an infinite chain. The disjoint blocks A_1 and A_2 have been taken with the same size $\ell_1 = \ell_2 \equiv \ell$, while the size of the block B_1 separating them is d. Thus, the four point ratio (43) becomes

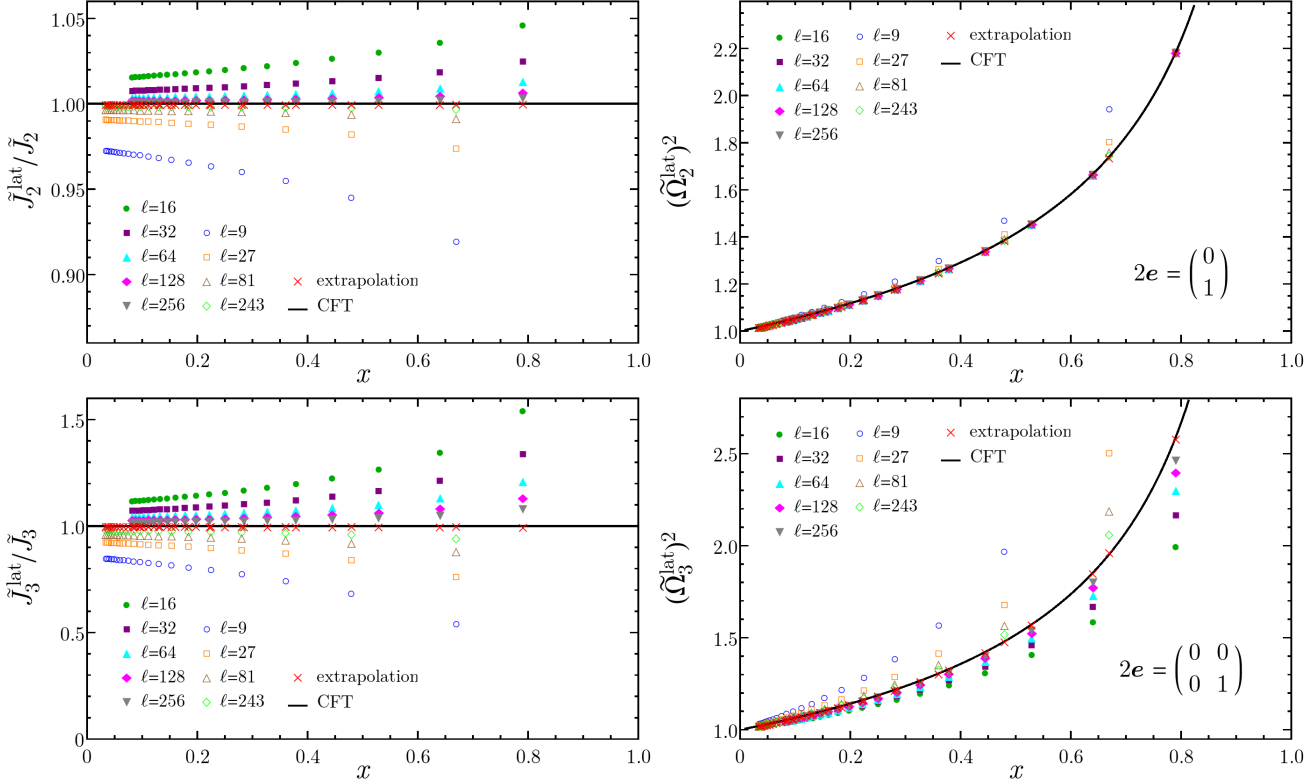$$x = \left(\frac{\ell}{\ell+d}\right)^2, \qquad (61)$$

Figure 3. The terms occurring in $\mathrm{Tr}(\rho_A^{T_2})^n$ for the free fermion (see (55)), according to the correspondence (52). Here we show $n = 2$ (top panels) and $n = 3$ (bottom panels). For each group of identical terms, only one representative has been plotted. In the left panels, the term with $\boldsymbol{p} = \boldsymbol{0}$ has been divided by its CFT counterpart ($\boldsymbol{\delta} = \boldsymbol{0}$), in order to simplify the residual dependence on ℓ_1 and ℓ_2. The extrapolated points (red crosses) are obtained through a fit of the data according to the scaling function (64) and they agree with the CFT predictions (solid lines).

and configurations with the same value of ℓ/d correspond to the same x.

Referring to Eq. (14), let us introduce the following lattice quantities

$$\tilde{J}_n^{\mathrm{lat}} = \mathrm{Tr}\tilde{\rho}_0^n, \qquad \widetilde{\Omega}_n^{\mathrm{lat}}[\boldsymbol{p}]^2 = \frac{1}{\mathrm{Tr}\tilde{\rho}_0^n} \, \mathrm{Tr}\left[\tilde{\rho}_0 \prod_{k=1}^{n-1} \tilde{\rho}_{p_k}\right], \tag{62}$$

which can be evaluated as explained in [59]. We also introduce their CFT continuum limit:

$$\tilde{J}_n \equiv c_n^2 \left(\frac{1-x}{\ell_1 \ell_2}\right)^{2\Delta_n}, \qquad \widetilde{\Omega}_n[\boldsymbol{e}] \equiv \left|\frac{\Theta[\boldsymbol{e}](\tilde{\tau}(x))}{\Theta(\tilde{\tau}(x))}\right|. \tag{63}$$

These CFT values are approached by taking configurations with increasing ℓ, keeping the ratio ℓ/d fixed. As discussed in Sec. 3.2.1, many terms in the sum (14) are equal because of the properties of the trace (in the continuum, this degeneracy is due to the dihedral symmetry of the Riemann surface).

In order to deal with the finite size effects, we perform an accurate scaling analysis, as done in [60] for $\mathrm{Tr}\rho_A^n$ and in [59] for $\mathrm{Tr}(\rho_A^{T_2})^n$. From general CFT arguments it has been
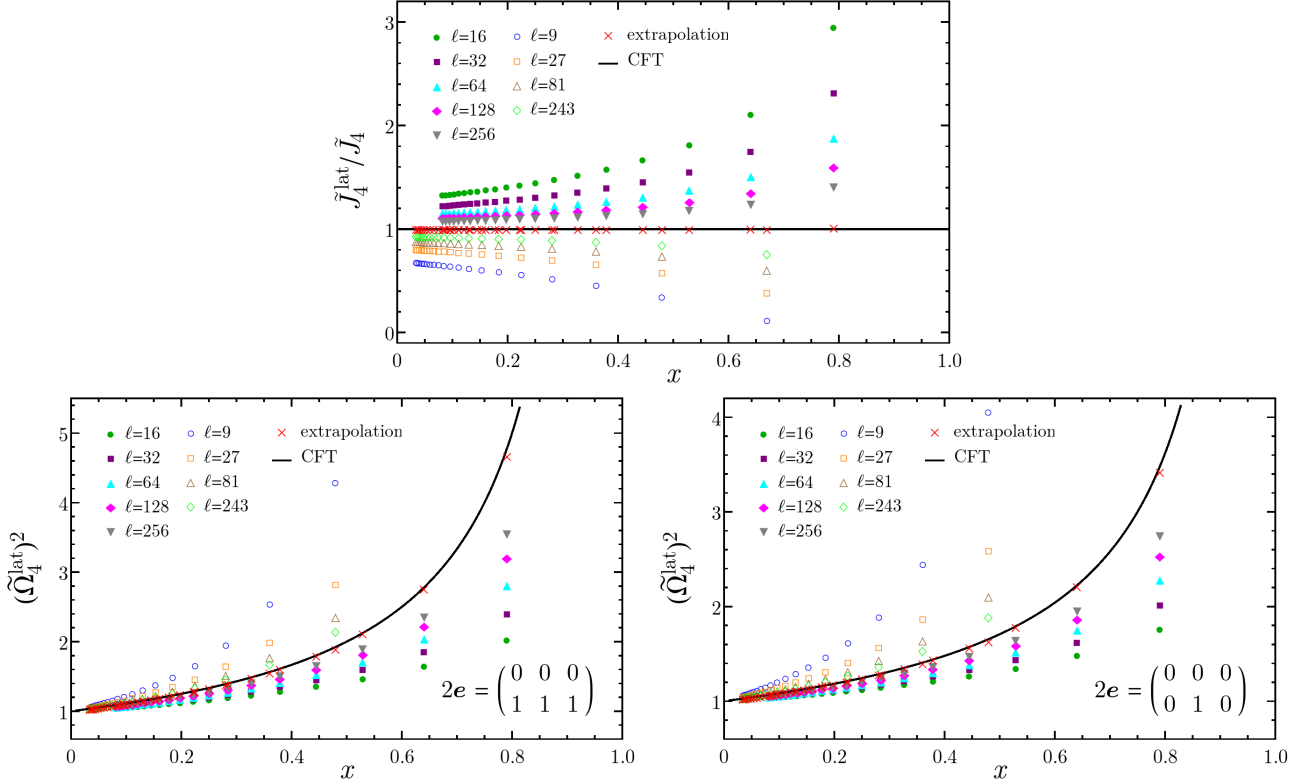
Figure 4. The terms occurring in $\text{Tr}(\rho_A^{T_2})^4$ for the free fermion (see (55)), according to the correspondence (52). For each of the three groups of identical terms, only one representative has been plotted. In the top panel, the term with $\boldsymbol{p} = \boldsymbol{0}$ has been divided by its CFT counterpart ($\boldsymbol{\delta} = \boldsymbol{0}$), in order to simplify the residual dependence on ℓ_1 and ℓ_2. The extrapolated points (red crosses) are obtained through a fit of the data according to the scaling function (64) and they agree with the CFT predictions (solid lines).

shown that these quantities display some unusual corrections to the scaling in ℓ described by a power law term with exponent $\delta_n = 2h/n$, being h the smallest scaling dimension of a relevant operator inserted at the branch points [65, 66, 67, 68]. For the Dirac fermion $h = 1$ and terms of the form $\ell^{-2m/n}$ are present, for any positive integer m. Because of the slow convergence of these terms (which becomes slower and slower for increasing n), typically it is necessary to include in the scaling function many of them. The most general finite-ℓ ansatz for $\widetilde{\Omega}_n$ takes the following form

$$\widetilde{\Omega}_n^{\text{lat}}[\boldsymbol{p}]^2 = \widetilde{\Omega}_n^2[\boldsymbol{e}] + \frac{\omega_n^{(1)}(x)}{\ell^{2/n}} + \frac{\omega_n^{(2)}(x)}{\ell^{4/n}} + \frac{\omega_n^{(3)}(x)}{\ell^{6/n}} + \ldots, \tag{64}$$

where $\widetilde{\Omega}[\boldsymbol{e}]$ is defined in (63) and $\boldsymbol{p}$ and $\boldsymbol{e}$ are related through (53) and (54). For the $\tilde{J}_n^{\text{lat}}/\tilde{J}_n$, a scaling function similar to (64) can be studied. Fitting the data with (64), the more terms we include, the more precise the fit could be. Nevertheless, since we have access to limited values of ℓ, by using too many terms overfitting problems may be encountered, which lead to very unstable results. The number of terms to be included in (64) has been chosen in order to get stable fits. We find that every term $\widetilde{\Omega}_n[\boldsymbol{e}]$ follows the

scaling (64) and the extrapolated value agrees with the corresponding CFT result.

Our numerical results are shown in Fig. 3 for $n = 2$ (top panels) and $n = 3$ (bottom panels), while Fig. 4 is about the $n = 4$ case. As for the prefactor, the ratio $\tilde{J}_n^{\text{lat}}/\tilde{J}_n$ has been considered in order to eliminate the trivial dependence on ℓ which survives in the continuum limit. The solid lines are the CFT predictions, which are given by (52).

4. Conclusions

In this manuscript we studied the moments of the partial transpose of the reduced density matrix $\text{Tr}(\rho_A^{T_2})^n$ for two disjoint intervals in the conformal field theory of the massless Dirac fermion. Our main result is a closed analytic form for these moments of arbitrary order, i.e. Eq. (55). For $n = 3, 4, 5$ this formula was anticipated in Ref. [59], but we extend here to arbitrary n and provide its full derivation. The analytic computation of the logarithmic negativity $\mathcal{E}$ through the replica limit of (55) for even $n_e \to 1$ is beyond our knowledge.

It turned out that these moments are identical, for arbitrary order, to those of the compactified boson at the self-dual point. This equality comes from the explicit computation and we miss a proper understanding of this fact. It was already noticed that for the moments of the reduced density matrix of two disjoint intervals $\text{Tr}\rho_A^n$, the result for the free fermion [41, 69] and the one for the compactified boson at the self-dual radius [38] are equal and very easy (they are both given by (42) with $\mathcal{F}_n(x) = 1$). This is not the case for three or more disjoint intervals [45, 46]. This unexpected equivalence has been investigated in [45], where also other results have been found, based on the fact that $\tau(x)$ is purely imaginary when $x \in (0, 1)$. For the partial transpose, the period matrix $\tilde{\tau}(x)$ of $\widetilde{\mathcal{R}}_n$ in (50) has a non vanishing real part. Nevertheless, here we have shown that $\text{Tr}\left(\rho_A^{T_2}\right)^n$ for the free fermion is equal to the one for the self-dual boson, a property that does not follow from the analysis of [45]. The equality of all the moments obviously implies also the equality of the negativities. Since the negativity is directly measurable by means of tensor network algorithms (as e.g. done in [21, 7] for the Ising model), it would be very interesting to check numerically the identity between the negativity of the tight-binding model and the isotropic Heisenberg antiferromagnet (whose continuum limit is the self-dual boson). This is a highly non trivial prediction.

We point out that an interesting technical byproduct of this paper is a one-to-one correspondence between each of the 2^{n-1} terms appearing in the lattice formulation of the moments $\text{Tr}(\rho_A^{T_2})^n$ and the partition function of the free fermion on $\widetilde{\mathcal{R}}_n$ with a particular assignment of fermionic boundary conditions. This correspondence has been explicitly checked against lattice numerical computations extending the numerical analysis of Ref. [59] where only the overall sum was considered. The consequence of this correspondence for the moments of both the reduce density matrix and its partial transpose in spin models with a free fermionic representation will be explored elsewhere [70].

Acknowledgments

Appendices

A. Reduced density matrix and its partial transpose on the lattice

In this appendix we briefly review the main tools employed in this manuscript to study the partial transpose for free fermions on the lattice.

Given the reduced density matrix (7), it is convenient to distinguish the terms having an even or odd number of fermionic operators in A_2 (notice that the parity of operator in A_2 is the same of the operators in A_1) by introducing

$$\rho_{\text{even}} = \frac{1}{2^{\ell_1+\ell_2}} \sum_{\text{even}} w_{12} \, O_1 O_2, \qquad \rho_{\text{odd}} = \frac{1}{2^{\ell_1+\ell_2}} \sum_{\text{odd}} w_{12} \, O_1 O_2. \qquad (65)$$

Thus $\rho_A = \rho_{\text{even}} + \rho_{\text{odd}}$. The partial transposition with respect to A_2 in (10) acts differently on the two operators in (65). In particular [26]

$$\rho_{\text{even}}^{T_2} = \frac{1}{2^{\ell_1+\ell_2}} \sum_{\text{even}} (-1)^{\mu_2/2} w_{12} \, O_1 O_2, \qquad \rho_{\text{odd}}^{T_2} = \frac{1}{2^{\ell_1+\ell_2}} \sum_{\text{odd}} (-1)^{(\mu_2-1)/2} w_{12} \, O_1 O_2. \quad (66)$$

Defining the following Gaussian matrix $\tilde{\rho}_A$ (which is not a density matrix, being not hermitian)

$$\tilde{\rho}_A = \frac{1}{2^{\ell_1+\ell_2}} \sum \mathrm{i}^{\mu_2} w_{12} \, O_1 O_2, \qquad (67)$$

and also $\tilde{\rho}_{\text{even}}$ and $\tilde{\rho}_{\text{odd}}$ as done in (65) for ρ_A, the partial transpose of ρ_A becomes

$$\rho_A^{T_2} = \tilde{\rho}_{\text{even}} - \mathrm{i}\,\tilde{\rho}_{\text{odd}}. \qquad (68)$$

The matrices $\tilde{\rho}_{\text{even}}$ and $\tilde{\rho}_{\text{odd}}$ in (68) can be written through the string P_{A_2} of the Majorana operator along A_2. Since $P_{A_2} a_j^{x,y} P_{A_2} = (-1)^{\delta_{j \in A_2}} a_j^{x,y}$, one finds

$$\tilde{\rho}_{\text{even}} = \frac{1}{2}\big(\tilde{\rho}_A + P_{A_2}\tilde{\rho}_A P_{A_2}\big), \qquad \tilde{\rho}_{\text{odd}} = \frac{1}{2}\big(\tilde{\rho}_A - P_{A_2}\tilde{\rho}_A P_{A_2}\big). \qquad (69)$$

Thus, plugging (69) into (68), the final expression for $\rho_A^{T_2}$ in (12) is obtained [26].

B. A check for $n = 2$

In this appendix, by employing the formalism described in Sec. 2.2 and Sec. 2.3, we check the standard relation between the reduced density matrix of two disjoint intervals and its partial transpose

$$\text{Tr}\left(\rho_A^{T_2}\right)^2 = \text{Tr}\left(\rho_A^2\right). \tag{70}$$

From (12), it is immediate to observe that $\text{Tr}\left(\rho_A^{T_2}\right)^2 = \text{Tr}\left(\tilde{\rho}_A P_{A_2} \tilde{\rho}_A P_{A_2}\right)$. Then, by using (18), we can write

$$
\begin{aligned}
\text{Tr}\left(\tilde{\rho}_A P_{A_2} \tilde{\rho}_A P_{A_2}\right) &= \hspace{12cm} (71) \\
&= \int D\zeta^* D\zeta \, D\eta^* D\eta \, e^{-\zeta^*\zeta} e^{-\eta^*\eta} \langle -\zeta_1, -\zeta_2 | \tilde{\rho}_A | \eta_1, \eta_2 \rangle \langle \eta_1, \eta_2 | P_{A_2} \tilde{\rho}_A P_{A_2} | \zeta_1, \zeta_2 \rangle \\
&= \int D\zeta^* D\zeta \, D\eta^* D\eta \, e^{-\zeta^*\zeta} e^{-\eta^*\eta} \langle -\zeta_1, -\zeta_2 | \tilde{\rho}_A | \eta_1, \eta_2 \rangle \langle \eta_1, -\eta_2 | \tilde{\rho}_A | \zeta_1, -\zeta_2 \rangle \\
&= \int D\zeta^* D\zeta \, D\eta^* D\eta \, e^{-\zeta^*\zeta} e^{-\eta^*\eta} \langle -\zeta_1, \eta_2^* | \rho_A | \eta_1, \zeta_2^* \rangle \langle \eta_1, -\zeta_2^* | \rho_A | \zeta_1, \eta_2^* \rangle \\
&= \int D\zeta^* D\zeta \, D\eta^* D\eta \, e^{-\zeta_1^*\zeta_1 + \zeta_2^*\zeta_2} e^{-\eta_1^*\eta_1 + \eta_2^*\eta_2} \langle -\zeta_1, \eta_2 | \rho_A | \eta_1, \zeta_2 \rangle \langle \eta_1, -\zeta_2 | \rho_A | \zeta_1, \eta_2 \rangle,
\end{aligned}
$$

where in the last step the change of variables $\zeta_2 \to \zeta_2^*$, $\eta_2 \to \eta_2^*$ has been employed. Then, by noticing that the relations in (18) can be slightly modified as follows

$$-\mathbb{I} = \int d\zeta^* d\zeta \, e^{\zeta^*\zeta} |\zeta\rangle \langle -\zeta|, \qquad -\text{Tr}\,\hat{O} = \int d\zeta^* d\zeta \, e^{\zeta^*\zeta} \langle \zeta | \hat{O} | \zeta \rangle, \tag{72}$$

we can conclude that (72) is exactly $\text{Tr}\left(\rho_A^2\right)$.

C. On the Riemann surface $\widetilde{\mathcal{R}}_n$

In this appendix we derive with all the details some results about the Riemann surface $\widetilde{\mathcal{R}}_n$ and its period matrix $\tilde{\tau}(x)$ in (50) that are employed in the main text.

Given the two disjoint intervals $A_1 = (u_1, v_1)$ and $A_2 = (u_2, v_2)$ whose endpoints are ordered as $u_1 < v_1 < u_2 < v_2$, $\text{Tr}\rho_A^n$ is the partition function of the model on the Riemann surface $\mathcal{R}_n$ which is defined by the following algebraic curve in $\mathbb{C}^2$ (parameterised by the complex variables z and y) [38]

$$y^n = (z - u_1)(z - u_2)\big[(z - v_1)(z - v_2)\big]^{n-1}. \tag{73}$$

The Riemann surface $\mathcal{R}_n$, which is an n sheeted cover of the complex plane, has genus $n - 1$ and it has been studied in detail in [71, 46], where its generalisation to any number of disjoint intervals (whose genus is $(n-1)(N-1)$ for N intervals) has been also discussed. By going around u_1 and u_2 clockwise, one goes from the j-th to the $(j+1)$-th sheet, while going around v_1 and v_2 clockwise, one moves to the $(j-1)$-th one.

In order to compute $\text{Tr}(\rho_A^{T_2})^n$, one has to find the partition function of the model on a different Riemann surface $\widetilde{\mathcal{R}}_n$, which is obtained by exchanging $u_2 \leftrightarrow v_2$ in (73), i.e.

$$y^n = (z - u_1)(z - v_2)\big[(z - v_1)(z - u_2)\big]^{n-1}. \tag{74}$$

The Riemann surface $\widetilde{\mathcal{R}}_n$ has genus $n-1$ and the sheets are joined in a different way with respect to $\mathcal{R}_n$. Indeed, by encircling u_2 clockwise we move from the j-th to the $(j-1)$-th sheet while by encircling v_2 clockwise the $(j+1)$-th sheet is reached.

While the period matrix $\tau(x)$ of $\mathcal{R}_n$ is purely imaginary (see (45)), the period matrix $\tilde{\tau}(x)$ for $\widetilde{\mathcal{R}}_n$ has a non vanishing real part. In Sec. C.1 we show that $\mathrm{Re}[\tilde{\tau}(x)]$ has a very simple form. In Sec. C.2 we consider the moments $\mathrm{Tr}\left(\rho_A^{T_2}\right)^n$ in the regime of small intervals $x \to 0$ and in Sec. C.3 we provide a detailed discussion of the $\mathbb{Z}_2$ part of the dihedral symmetry for $\widetilde{\mathcal{R}}_n$.

C.1. The real and imaginary part of the period matrix $\tilde{\tau}(x)$

In this subsection we want to write explicitly the real and the imaginary part of the period matrix $\tilde{\tau}(x)$ given by (50). The real part $\mathrm{Re}[\tilde{\tau}(x)]$ turns out to be a simple tridiagonal matrix with half-integer entries.

Let us introduce the following ratios of hypergeometric functions, which enter in the expressions for the period matrices $\tau(x)$ and $\tilde{\tau}(x)$ (see (45) and (50))

$$\tau_r(x) \equiv \mathrm{i}\,\frac{{}_2F_1(r, 1-r; 1; 1-x)}{{}_2F_1(r, 1-r; 1; x)}, \qquad \tilde{\tau}_r(x) \equiv \tau_r\left(\frac{x}{x-1}\right) \equiv \tilde{\alpha}_r(x) + \mathrm{i}\tilde{\beta}_r(x), \qquad (75)$$

where $0 < r < 1$ and $x \in (0,1)$. Moreover, we also define

$$\mathcal{A}_r(x) \equiv \frac{\Gamma(1-2r)}{\Gamma(1-r)^2}\,\frac{{}_2F_1(r, r; 2r; 1-x)}{{}_2F_1(r, r; 1; x)}, \qquad (76)$$

$$\mathcal{B}_r(x) \equiv \frac{\Gamma(2r-1)}{\Gamma(r)^2}\,(1-x)^{1-2r}\,\frac{{}_2F_1(1-r, 1-r; 2(1-r); 1-x)}{{}_2F_1(r, r; 1; x)}. \qquad (77)$$

By employing the expressions given in (87) of [6], one finds that

$$\tilde{\alpha}_r(x) = \sin(\pi r)\big[\mathcal{A}_r(x) + \mathcal{B}_r(x)\big], \qquad \tilde{\beta}_r(x) = \cos(\pi r)\big[\mathcal{A}_r(x) - \mathcal{B}_r(x)\big]. \qquad (78)$$

At this point we need the following identity (see e.g. Eq. (1) at pag. 108 of Ref. [72])

$$
\begin{aligned}
{}_2F_1(a, b; c; z) &= \frac{\Gamma(c)\,\Gamma(c-a-b)}{\Gamma(c-a)\,\Gamma(c-b)}\,{}_2F_1(a, b; a+b-c+1; 1-z) \\
&\quad + \frac{\Gamma(c)\,\Gamma(a+b-c)}{\Gamma(a)\,\Gamma(b)}\,(1-z)^{c-a-b}\,{}_2F_1(c-a, c-b; c-a-b+1; 1-z),
\end{aligned}
\qquad (79)
$$

which holds for $|\arg(1-z)| < \pi$. By specialising (79) to the case of $(a, b, c) = (r, r, 1)$ and $z = x \in (0,1)$, from (76) and (77) one finds that

$$\mathcal{A}_r(x) + \mathcal{B}_r(x) = 1. \qquad (80)$$

From this expression it is clear that the x dependence disappears from the real part of $\tilde{\tau}_r(x)$ and hence from the period matrix. Indeed, using (78) and (80) in (45) one gets (see also (50))

$$\tilde{\tau}(x)_{i,j} = \frac{2}{n}\sum_{k=1}^{n-1}\sin(\pi k/n)\,\tilde{\tau}_{k/n}(x)\,\cos[2\pi(k/n)(i-j)] = \frac{1}{2}\big[\mathcal{Q}\big]_{i,j} + \mathrm{i}\,\big[\mathcal{I}(x)\big]_{i,j}, \qquad (81)$$

where the sum giving the real part can be explicitly performed, finding that the matrix $\mathcal{Q}$ has integer elements which read

$$[\mathcal{Q}]_{i,j} \equiv 2\delta_{i,j} - \delta_{|i-j|,1}, \tag{82}$$

namely $\mathcal{Q}$ is a symmetric tridiagonal matrix, with 2 on the main diagonal and -1 on the first diagonals. On the other hand, the imaginary part can be written as follows,

$$\left[\mathcal{I}(x)\right]_{i,j} = \frac{2}{n} \sum_{k=1}^{n-1} \sin(\pi k/n)\, \tilde{\beta}_{k/n}(x) \cos[2\pi(k/n)(i-j)], \tag{83}$$

with

$$\tilde{\beta}_r(x) \equiv \frac{\tilde{f}_r(1-x) - \tilde{f}_{1-r}(1-x)}{(1-x)^r \, {}_2F_1(r,r;1;x)}\, \cos(\pi r), \qquad \tilde{f}_r(x) \equiv \frac{\Gamma(1-2r)}{\Gamma(1-r)^2}\, x^r \, {}_2F_1(r,r;2r;x). \tag{84}$$

This expression for $\mathcal{I}(x)$ can be further simplified. Plugging (80) into the second expression of (78), we have

$$\tilde{\beta}_r(x) = \cos(\pi r)\big[2\mathcal{A}_r(x) - 1\big]. \tag{85}$$

For $0 < x < 1$ we can rewrite $\mathcal{A}_r(x)$ as follows [72]

$$\mathcal{A}_r(x) = \frac{1}{2\cos(\pi r)}\left[e^{-\mathrm{i}\pi r} + e^{\mathrm{i}\pi r}\, x^{-r}\, \frac{{}_2F_1(r,r;1;1/x)}{{}_2F_1(r,r;1;x)}\right]. \tag{86}$$

Since $\mathcal{A}_r(x)$ is real for $0 < x < 1$, the vanishing of its imaginary part gives

$$\frac{1}{x^r}\left[\tan(\pi r)\,\mathrm{Re}\left(\frac{{}_2F_1(r,r;1;1/x)}{{}_2F_1(r,r;1;x)}\right) + \mathrm{Im}\left(\frac{{}_2F_1(r,r;1;1/x)}{{}_2F_1(r,r;1;x)}\right)\right] = \tan(\pi r). \tag{87}$$

On the other hand, by writing $\mathcal{A}_r(x)$ as its real part and plugging the resulting expression in (85), one finds

$$\tilde{\beta}_r(x) = \frac{1}{x^r}\left[\cos(\pi r)\,\mathrm{Re}\left(\frac{{}_2F_1(r,r;1;1/x)}{{}_2F_1(r,r;1;x)}\right) - \sin(\pi r)\,\mathrm{Im}\left(\frac{{}_2F_1(r,r;1;1/x)}{{}_2F_1(r,r;1;x)}\right)\right]. \tag{88}$$

Finally, using (87) we can write

$$\tilde{\beta}_r(x) = \cos(\pi r) - \frac{x^{-r}}{\sin(\pi r)}\,\mathrm{Im}\left(\frac{{}_2F_1(r,r;1;1/x)}{{}_2F_1(r,r;1;x)}\right). \tag{89}$$

The matrix $\mathcal{I}(x)$ can be easily written by plugging (89) into (83) and noticing that the sum over the cosine vanishes. The result reads

$$\left[\mathcal{I}(x)\right]_{i,j} = -\frac{2}{n}\sum_{k=1}^{n-1} x^{-k/n}\,\mathrm{Im}\left(\frac{{}_2F_1(k/n,k/n;1;1/x)}{{}_2F_1(k/n,k/n;1;x)}\right)\cos[2\pi(k/n)(i-j)]. \tag{90}$$

The result (82) is employed in Sec. 3.3 and in App. C.3.

C.2. Short intervals regime

In this appendix we study the $\mathrm{Tr}\left(\rho_A^{T_2}\right)^n$ for the free fermion (55) in the limit of short intervals, i.e. when $x \to 0$.

In the expression (55), only Riemann theta functions with $\boldsymbol{\varepsilon} = \mathbf{0}$ occur, which are given by

$$\Theta\begin{bmatrix}\mathbf{0}\\\boldsymbol{\delta}\end{bmatrix}(\tilde{\tau}(x)) = 1 + \sum_{\boldsymbol{m}\neq\mathbf{0}} e^{i\pi(\boldsymbol{m}\cdot\mathcal{Q}\cdot\boldsymbol{m}+2\boldsymbol{\delta}\cdot\boldsymbol{m})}\, e^{-\pi\,\boldsymbol{m}\cdot\mathcal{I}\cdot\boldsymbol{m}}, \tag{91}$$

where $\mathcal{Q}$ is independent of x. Expanding $\tilde{\beta}_{k/n}(x)$ in (84) for $x \to 0$, one finds

$$\tilde{\beta}_q(x) = -\frac{\sin(\pi q)}{\pi}\left[\log(x) + 2\gamma_E + \psi(q) + \psi(1-q)\right] + O(x). \tag{92}$$

Plugging this expansion into (83) and (91), one gets that the leading term is $x^{\boldsymbol{m}\cdot\mathcal{Q}\cdot\boldsymbol{m}}$. The exponent $\boldsymbol{m}\cdot\mathcal{Q}\cdot\boldsymbol{m}$ for $\boldsymbol{m}\in\mathbb{Z}^{n-1}$ has been already analyzed in [39], finding that its minimum is 1, which is obtained for the following vectors

$$\boldsymbol{m}_\pm \equiv (\,\overbrace{\underbrace{0,\ldots,0}_{j_1},\pm 1,\ldots,\pm 1}^{j_2}, 0,\ldots,0\,), \qquad \boldsymbol{m}_\pm \neq \mathbf{0}, \qquad 0 \leqslant j_1 < j_2 \leqslant n-1, \tag{93}$$

namely $\boldsymbol{m}_\pm \cdot \mathcal{Q} \cdot \boldsymbol{m}_\pm = 1$. Then, by applying again the results of [39] (notice that the vectors $\boldsymbol{m}_+$ and $\boldsymbol{m}_-$ give the same contribution) to (91), we find

$$\Theta\begin{bmatrix}\mathbf{0}\\\boldsymbol{\delta}\end{bmatrix}(\tilde{\tau}(x)) = 1 - \frac{x}{2n^2}\sum_{\boldsymbol{m}_+}\frac{(-1)^{2\boldsymbol{\delta}\cdot\boldsymbol{m}_+}}{\sin^2(\pi(j_2-j_1)/n)} + \ldots, \tag{94}$$

where the dots denote $o(x)$ terms. Thus, for the generic term occurring in the sum (55) we have

$$\widetilde{\Omega}_n[\boldsymbol{e}] = 1 - \frac{x}{2n^2}\sum_{\boldsymbol{m}_+}\frac{1 + (-1)^{2\boldsymbol{\delta}\cdot\boldsymbol{m}_+}}{\sin^2(\pi(j_2-j_1)/n)} + \ldots, \qquad \boldsymbol{e} = \begin{pmatrix}\mathbf{0}\\\boldsymbol{\delta}\end{pmatrix}. \tag{95}$$

Plugging this result into (55), we get the first term of the $x \to 0$ expansion of $\mathrm{Tr}\left(\rho_A^{T_2}\right)^n$, which is

$$\mathrm{Tr}\left(\rho_A^{T_2}\right)^n = \tilde{J}_n\left[1 - \frac{x}{2^{n-1}\,n^2}\sum_{\boldsymbol{\delta}}r_n(\boldsymbol{\delta})\sum_{\boldsymbol{m}_+}\frac{1 + (-1)^{2\boldsymbol{\delta}\cdot\boldsymbol{m}_+}}{\sin^2(\pi(j_2-j_1)/n)} + \ldots\right]. \tag{96}$$

C.3. The $\mathbb{Z}_2$ part of the dihedral symmetry of $\widetilde{\mathcal{R}}_n$

In this subsection we briefly discuss the most peculiar aspect of the dihedral symmetry for the Riemann surface $\widetilde{\mathcal{R}}_n$ occurring in the computation of $\mathrm{Tr}\left(\rho_A^{T_2}\right)^n$ (see Sec. 3.2.1).

The Riemann surface $\mathcal{R}_n$ has a dihedral symmetry $\mathbb{Z}_n \times \mathbb{Z}_2$ due to the invariance under cyclic permutation of the sheets ($\mathbb{Z}_n$) and the complex conjugation ($\mathbb{Z}_2$). For a genus g Riemann surface, the modular transformations are given by the symplectic matrices $Sp(2g, \mathbb{Z})$ [56, 57]. The dihedral symmetry can be identified with a subgroup

of the modular transformations acting on $\mathcal{R}_n$ which has been discussed in [45, 46]. In particular, these peculiar modular transformations map the a cycles among themselves and the b cycles among themselves, leaving the period matrix $\tau(x)$ unchanged.

Also the surface $\widetilde{\mathcal{R}}_n$ has a dihedral symmetry $\mathbb{Z}_n \times \mathbb{Z}_2$ but, while the cyclic permutation ($\mathbb{Z}_n$) is exactly the same one discussed above for $\mathcal{R}_n$, the complex conjugation is slightly different because it mixes a and b cycles. Let us remind that the complex conjugation corresponds to reverse the order of the sheets and to reflect all of them with respect to the real axis. Considering the canonical homology basis $\{\tilde{a}_r, \tilde{b}_r; 1 \leqslant r \leqslant n-1\}$ introduced in Sec. 3.2 (see Fig. 2) [46], this transformation acts as follows

$$\begin{pmatrix} \tilde{\boldsymbol{a}}' \\ \tilde{\boldsymbol{b}}' \end{pmatrix} = M_{\text{inv}} \cdot \begin{pmatrix} \tilde{\boldsymbol{a}} \\ \tilde{\boldsymbol{b}} \end{pmatrix}, \qquad M_{\text{inv}} = \begin{pmatrix} \overset{\leftrightarrow}{\mathbb{I}}_{n-1} & 0 \\ -\overset{\leftrightarrow}{\mathcal{Q}} & \overset{\leftrightarrow}{\mathbb{I}}_{n-1} \end{pmatrix} \in Sp\big(2(n-1), \mathbb{Z}\big), \tag{97}$$

where we introduced the notation of the double-headed arrow above a matrix to indicate that the columns have to be taken in the reversed order ($\mathbb{I}_k$ is the $k \times k$ identity matrix and $\mathcal{Q}$ is given by (82)). Under the symplectic transformation defined in (97), the period matrix $\tilde{\tau}$ (50) changes as follows

$$\tilde{\tau}' = \overset{\leftrightarrow}{\mathbb{I}} \cdot \tilde{\tau} \cdot \overset{\leftrightarrow}{\mathbb{I}} - \overset{\leftrightarrow}{\mathcal{Q}} \cdot \overset{\leftrightarrow}{\mathbb{I}} = \tilde{\tau} - \mathcal{Q} = -\mathcal{R} + \mathrm{i}\mathcal{I} = -\tilde{\tau}^*, \tag{98}$$

while for the characteristics of the Riemann theta functions we have

$$\begin{pmatrix} \boldsymbol{\varepsilon}' \\ \boldsymbol{\delta}' \end{pmatrix} = \begin{pmatrix} \overset{\leftrightarrow}{\mathbb{I}} & 0 \\ \overset{\leftrightarrow}{\mathcal{Q}} & \overset{\leftrightarrow}{\mathbb{I}} \end{pmatrix} \cdot \begin{pmatrix} \boldsymbol{\varepsilon} \\ \boldsymbol{\delta} \end{pmatrix}. \tag{99}$$

Notice that the powers of M_{inv} read

$$M_{\text{inv}}^{2k-1} = \begin{pmatrix} \overset{\leftrightarrow}{\mathbb{I}} & 0 \\ -(2k-1)\overset{\leftrightarrow}{\mathcal{Q}} & \overset{\leftrightarrow}{\mathbb{I}} \end{pmatrix}, \qquad M_{\text{inv}}^{2k} = \begin{pmatrix} \mathbb{I} & 0 \\ -2k\mathcal{Q} & \mathbb{I} \end{pmatrix}, \tag{100}$$

(in particular, notice that $M_{\text{inv}}^2 \neq \mathbb{I}$) so that, by applying (98) k times one finds

$$\tilde{\tau}^{(k)} = \tilde{\tau} - k\,\mathcal{Q}. \tag{101}$$

As for the change of the Riemann theta function under the modular transformation in (97), because of the particular form of $\mathcal{Q}$, it is easy to show that for k even it is left invariant (a part for an overall sign), while for k odd it becomes its complex conjugate, up to an overall sign. Since in our formulas the modulus of the Riemann theta function always occurs, the terms occurring in our sum over the characteristics are invariant under this transformation. Thus, M_{inv} can be the modular transformation representing the $\mathbb{Z}_2$ of the dihedral symmetry, even if $M_{\text{inv}}^2 \neq \mathbb{I}$.

D. Details on the computation for the self-dual boson

In this appendix we show the equality $m_n(\boldsymbol{\delta}) = r_n(\boldsymbol{\delta})$ between the coefficient $m_n(\boldsymbol{\delta})$ in (60), coming from the self-dual boson approach, and the coefficient $r_n(\boldsymbol{\delta})$ in (56) occurring in the expression obtained through the free fermion analysis.

Considering $m_n(\boldsymbol{\delta})$ in (60), the expression in the exponent can be written as follows

$$\boldsymbol{\varepsilon} \cdot \frac{\mathcal{Q}}{2} \cdot \boldsymbol{\varepsilon} + \boldsymbol{\varepsilon} \cdot \boldsymbol{\delta} = -\sum_{i=1}^{n-2} \varepsilon_i \varepsilon_{i+1} + \sum_{i=1}^{n-1} \varepsilon_i^2 + \sum_{i=1}^{n-1} \varepsilon_i \delta_i. \tag{102}$$

Then, defining the spin variables $\sigma_i = 4\varepsilon_i - 1 = \pm 1$ and local magnetic fields $h_i = 4\delta_i$, we find that $m_n(\boldsymbol{\delta})$ is equal to the partition function Z_n of $n-1$ Ising spins in a binary magnetic field $h_i = 0, 2$ (a part for the first and last site), which reads

$$Z_n = e^{\frac{i\pi}{4}\left(\sum_i h_i + n\right)} \sum_{\boldsymbol{\sigma}} \exp\left[i\frac{\pi}{4}\left(-\sum_{i=1}^{n-2} \sigma_i \sigma_{i+1} + \sum_{i=1}^{n-1} \sigma_i h_i + \sigma_1 + \sigma_{n-1}\right)\right]. \tag{103}$$

Given this Ising model representation, we can compute $m_n(\boldsymbol{\delta})$ through standard transfer matrix techniques. Following [73], let us introduce the conditioned partition function with the last spin set to μ, namely

$$Z_n(\mu) = e^{\frac{i\pi}{4}\left(\sum_i h_i + n\right)} \sum_{\boldsymbol{\sigma}} \exp\left[\frac{i\pi}{4}\left(-\sum_{i=1}^{n-3} \sigma_i \sigma_{i+1} - \mu \sigma_{n-2} + \sum_{i=1}^{n-2} \sigma_i h_i + \mu h_{n-1} + \sigma_1 + \mu\right)\right]. \tag{104}$$

Then, by adding one spin ϵ to the partition function, it becomes

$$Z_{n+1}(\epsilon) = e^{\frac{i\pi}{4}\left(\sum_i h_i + n\right)} \times \tag{105}$$

$$\times \sum_{\mu=\pm 1} \sum_{\boldsymbol{\sigma}} \exp\left[\frac{i\pi}{4}\left(-\sum_{i=1}^{n-3} \sigma_i \sigma_{i+1} - \mu \sigma_{n-2} - \mu \epsilon + \sum_{i=1}^{n-2} \sigma_i h_i + \mu h_{n-1} + \epsilon h_n + \sigma_1 + \epsilon\right)\right].$$

After some algebra, one realizes that

$$Z_{n+1}(+) = (-1)^{2\delta_n} \left[Z_n(+) - Z_n(-)\right], \qquad Z_{n+1}(-) = Z_n(+) + Z_n(-). \tag{106}$$

and these relations give the transfer matrix

$$\widehat{T}(\delta) = \frac{1}{\sqrt{2}} \begin{pmatrix} (-1)^{2\delta} & -(-1)^{2\delta} \\ 1 & 1 \end{pmatrix}, \qquad \delta \in \{0, 1/2\}. \tag{107}$$

We also need the conditioned partition functions for a single spin, which read

$$Z_2(+) = -e^{\frac{i\pi}{2}h_1}, \qquad Z_2(-) = 1. \tag{108}$$

Then, the partition function for $n-1$ spins in (103) is given by

$$Z_n = Z_n(+) + Z_n(-) = \tag{109}$$

$$= 2^{\frac{n}{2}-1} \begin{pmatrix} 1 & 1 \end{pmatrix} \prod_{k=n-1}^{2} \widehat{T}(\delta_k) \begin{pmatrix} -(-1)^{2\delta_1} \\ 1 \end{pmatrix} = 2^{\frac{n-1}{2}} \begin{pmatrix} 1 & 1 \end{pmatrix} \prod_{k=n-1}^{1} \widehat{T}(\delta_k) \begin{pmatrix} 0 \\ 1 \end{pmatrix}.$$

In order to compute the matrix product in (109), it is convenient to perform a change of basis which diagonalises $\widehat{T}(0)$, namely

$$T(\delta) = U^\dagger \, \widehat{T}(\delta) \, U, \qquad U = \frac{1}{2} \begin{pmatrix} 1+\mathrm{i} & -(1+\mathrm{i}) \\ 1-\mathrm{i} & 1-\mathrm{i} \end{pmatrix}. \tag{110}$$

From (107) and (110) we can explicitly write the transfer matrix in the new basis

$$T(0) = \frac{1}{\sqrt{2}} \begin{pmatrix} 1+\mathrm{i} & 0 \\ 0 & 1-\mathrm{i} \end{pmatrix}, \qquad T(1/2) = \frac{1}{\sqrt{2}} \begin{pmatrix} 0 & 1-\mathrm{i} \\ 1+\mathrm{i} & 0 \end{pmatrix}, \tag{111}$$

and therefore the partition function (109) can be rewritten as follows

$$Z_n = 2^{\frac{n}{2}-1} \begin{pmatrix} 1 & 1 \end{pmatrix} T(0) \prod_{k=n-1}^{1} T(\delta_k) \begin{pmatrix} 1 \\ 1 \end{pmatrix}. \tag{112}$$

Now, it is convenient to move all $T(0)$'s in the product of (112) to the left of all the $T(1/2)$'s. To do this, one observes that $T(0)T(1/2) = T(1/2)T(0)^{-1}$ and $T(1/2)T(0) = T(0)^{-1}T(1/2)$. By employing the latter rule, one finds

$$Z_n = 2^{\frac{n}{2}-1} \begin{pmatrix} 1 & 1 \end{pmatrix} T(0)^{1+\sum_i (1-2\delta_i)(-1)^{\sum_{j=i}^{n-1} 2\delta_j}} \, T(1/2)^{\sum_i 2\delta_i} \begin{pmatrix} 1 \\ 1 \end{pmatrix}. \tag{113}$$

The factor $1 - 2\delta_i$ within the sum in the exponent of $T(0)$ selects only the sites where $\delta_i = 0$, while the other factor $(-1)^{\sum_{j=i}^{n-1} 2\delta_j}$ counts all the $T(1/2)$'s on the left of site i. The exponent of $T(0)$ can be rewritten as

$$s(\boldsymbol{\delta}) = 1 + \sum_{i=1}^{n-1} (1-2\delta_i)(-1)^{\sum_{j=i}^{n-1} 2\delta_j} = 1 + \frac{1-(-1)^{\sum_i 2\delta_i}}{2} + \sum_{i=1}^{n-1} (-1)^{\sum_{j=i}^{n-1} 2\delta_j}. \tag{114}$$

Since $T(0)$ is diagonal, its powers can be easily performed. Moreover, since $T(1/2)^2 = \mathbb{I}_2$, every integer power of $T(1/2)$ is simply $\mathbb{I}_2$ if the exponent is even, and $T(1/2)$ otherwise. Thus, we have

$$T(0)^{s(\boldsymbol{\delta})} = \begin{pmatrix} e^{\frac{\mathrm{i}\pi}{4} s(\boldsymbol{\delta})} & 0 \\ 0 & e^{-\frac{\mathrm{i}\pi}{4} s(\boldsymbol{\delta})} \end{pmatrix}, \tag{115}$$

$$T(1/2)^{2\sum_i \delta_i} = \begin{pmatrix} [1+(-1)^{\sum_i 2\delta_i}]/2 & e^{-\frac{\mathrm{i}\pi}{4}}[1-(-1)^{\sum_i 2\delta_i}]/2 \\ e^{\frac{\mathrm{i}\pi}{4}}[1-(-1)^{\sum_i 2\delta_i}]/2 & [1+(-1)^{\sum_i 2\delta_i}]/2 \end{pmatrix}. \tag{116}$$

Finally, (113) tells us that we just need to multiply this two matrices and to sum the four elements of the resulting matrix. After some of algebra, we get

$$m_n(\boldsymbol{\delta}) = 2^{n/2} \left[\frac{1+(-1)^{\sum_i 2\delta_i}}{2} \cos\left(\frac{\pi}{4} s(\boldsymbol{\delta})\right) + \frac{1-(-1)^{\sum_i 2\delta_i}}{2} \cos\left(\frac{\pi}{4}\left(s(\boldsymbol{\delta})-1\right)\right) \right]. \tag{117}$$

By inspection of the two cases of $\sum_i 2\delta_i$ even or odd, it is clear that (117) equals (56).

References

[1] L. Amico, R. Fazio, A. Osterloh, and V. Vedral, Rev. Mod. Phys. **80**, 517 (2008);
    J. Eisert, M. Cramer, and M. B. Plenio, Rev. Mod. Phys. **82**, 277 (2010);
    P. Calabrese, J. Cardy, and B. Doyon Eds, J. Phys. A **42** 500301 (2009).

[2] A. Peres, Phys. Rev. Lett. **77**, 1413 (1996);
    K. Zyczkowski, P. Horodecki, A. Sanpera and M. Lewenstein, Phys. Rev. A **58**, 883 (1998);
    J. Eisert and M. B. Plenio, J. Mod. Opt. **46**, 145 (1999).

[3] G. Vidal and R. F. Werner, Phys. Rev. A **65**, 032314 (2002).

[4] J. Eisert, quant-ph/0610253;
    M. B. Plenio, Phys. Rev. Lett. **95**, 090503 (2005).

[5] P. Calabrese, J. Cardy, and E. Tonni, Phys. Rev. Lett. **109**, 130502 (2012).

[6] P. Calabrese, J. Cardy, and E. Tonni, J. Stat. Mech. P02008 (2013).

[7] P. Calabrese, L. Tagliacozzo and E. Tonni, J. Stat. Mech. P05002 (2013).

[8] M. Rangamani and M. Rota, JHEP 1410 (2014) 60;
    M. Kulaxizi, A. Parnachev, and G. Policastro, JHEP 1409 (2014) 010;
    E. Perlmutter, M. Rangamani, and M. Rota, arXiv:1506.01679.

[9] P. Calabrese, J. Cardy, and E. Tonni, J. Phys. A **48**, 015006 (2015).

[10] V. Eisler and Z. Zimboras, New J. Phys. **16**, 123020 (2014).

[11] A. Coser, E. Tonni and P. Calabrese, J. Stat. Mech. P12017 (2014).

[12] M. Hoogeveen and B. Doyon, Nucl. Phys. B **898**, 78 (2015).

[13] X. Wen, P.-Y. Chang, and S. Ryu, arXiv:1501.00568.

[14] C. Castelnovo, Phys. Rev. A **88**, 042319 (2013);
    C. Castelnovo, Phys. Rev. A **89**, 042333 (2014).

[15] Y. A. Lee and G. Vidal, Phys. Rev. A **88**, 042318 (2013).

[16] R. Santos, V. Korepin, and S. Bose, Phys. Rev. A **84**, 062307 (2011);
    R. Santos and V. Korepin, J. Phys. A **45**, 125307 (2012).

[17] C. M. Agón, M. Headrick, D. L. Jafferis, and S. Kasko, Phys. Rev. D **89**, 025018 (2014).

[18] C. De Nobili, A. Coser and E. Tonni, J. Stat. Mech. P06021 (2015).

[19] V. Alba, J. Stat. Mech. P05013 (2013).

[20] C. Chung, V. Alba, L. Bonnes, P. Chen, and A. Lauchli, Phys. Rev. B **90**, 064401 (2014).

[21] H. Wichterich, J. Molina-Vilaplana and S. Bose, Phys. Rev. A **80**, 010304 (2009).

[22] J. Anders and A. Winter, Quantum Inf. Comput. **8**, 0245 (2008);
    J. Anders, Phys. Rev. A **77**, 062102 (2008).

[23] A. Ferraro, D. Cavalcanti, A. Garcia-Saez, and A. Acin, Phys. Rev. Lett. **100**, 080502 (2008);
    D. Cavalcanti, A. Ferraro, A. Garcia-Saez, and A. Acin, Phys. Rev. A **78**, 012335 (2008).

[24] H. Wichterich, J. Vidal, and S. Bose, Phys. Rev. A **81**, 032311 (2010).

[25] A. Bayat, P. Sodano, and S. Bose, Phys. Rev. Lett. **105**, 187204 (2010);
    A. Bayat, P. Sodano, and S. Bose, Phys. Rev. B **81**, 064429 (2010);
    P. Sodano, A. Bayat, and S. Bose, Phys. Rev. B **81**, 100412 (2010);
    A. Bayat, S. Bose, P. Sodano, and H. Johannesson, Phys. Rev. Lett. **109**, 066403 (2012).

[26] V. Eisler and Z. Zimboras, New J. Phys. **17**, 053048 (2015).

[27] F. Igloi and I. Peschel, EPL **89**, 40001 (2010).

[28] V. Alba, L. Tagliacozzo, and P. Calabrese, Phys. Rev. B **81** 060411 (2010).

[29] G. Vidal, J. Latorre, E. Rico and A. Kitaev, Phys. Rev. Lett. **90**, 227902 (2003);
    J. I. Latorre, E. Rico, and G. Vidal, Quant. Inf. Comp. **4**, 048 (2004).

[30] H. Kleinert, *Path Integrals in Quantum Mechanics, Statistics, Polymer Physics, and Financial Markets*, World Scientific, 5th ed., 2009.

[31] C. Holzhey, F. Larsen, and F. Wilczek, Nucl. Phys. B **424**, 443 (1994);
    C. G. Callan and F. Wilczek, Phys. Lett. B **333**, 55 (1994).

[32] P. Calabrese and J. Cardy, J. Stat. Mech. P06002 (2004).

[33] P. Calabrese and J. Cardy, J. Phys. A **42**, 504005 (2009).

[34] M Fagotti, P Calabrese, and J E Moore, Phys. Rev. B **83**, 045110 (2011).

[35] J. Cardy, O. Castro-Alvaredo, and B. Doyon, J. Stat. Phys. **130**, 129 (2008).

[36] P. Calabrese and A. Lefevre, Phys. Rev. A **78**, 032329 (2008).

[37] B.-Q. Jin and V. E. Korepin, J. Stat. Phys. **116**, 79 (2004).

[38] P. Calabrese, J. Cardy, and E. Tonni, J. Stat. Mech. P11001 (2009).

[39] P. Calabrese, J. Cardy, and E. Tonni, J. Stat. Mech. P01021 (2011).

[40] M. Caraglio and F. Gliozzi, JHEP 0811: 076 (2008).

[41] H. Casini, C. D. Fosco, and M. Huerta, J. Stat. Mech. P05007 (2005).

[42] S. Furukawa, V. Pasquier, and J. Shiraishi, Phys. Rev. Lett. **102**, 170602 (2009).

[43] P. Calabrese, J. Stat. Mech. P09013 (2010).

[44] M. Headrick, Phys. Rev. D **82**, 126010 (2010).

[45] M. Headrick, A. Lawrence, and M. Roberts, J. Stat. Mech. P02022 (2013).

[46] A. Coser, L. Tagliacozzo, and E. Tonni, J. Stat. Mech. P01008 (2014).

[47] V. Alba, L. Tagliacozzo, and P. Calabrese, J. Stat. Mech. P06012 (2011).

[48] M. Rajabpour and F. Gliozzi, J. Stat. Mech. P02016 (2012).

[49] M. Fagotti, EPL **97**, 17007 (2012).

[50] B. Chen and J. Zhang, JHEP 1311 (2013) 164.

[51] S. Ryu and T. Takayanagi, Phys. Rev. Lett. **96**, 181602 (2006);
S. Ryu and T. Takayanagi, JHEP 0608: 045 (2006);
T. Nishioka, S. Ryu, and T. Takayanagi, J. Phys. A **42**, 504008 (2009).

[52] V. E. Hubeny and M. Rangamani, JHEP 0803: 006 (2008);
E. Tonni, JHEP 1105:004 (2011);
P. Hayden, M. Headrick and A. Maloney Phys. Rev. D **87**, 046003 (2013);
T. Faulkner, arXiv:1303.7221;
T. Hartman, arXiv:1303.6955;
T. Faulkner, A. Lewkowycz, and J. Maldacena, JHEP 1311 (2013) 074;
P. Fonda, L. Giomi, A. Salvio and E. Tonni, JHEP 1502 (2015) 005.

[53] J. Cardy, J. Phys. A **46** 285402 (2013);
H. Casini and M. Huerta, JHEP 0903: 048 (2009);
H. Casini and M. Huerta, Class. Quant. Grav. **26**, 185005 (2009);
N. Shiba, JHEP 1207:100 (2012);
L.-Y. Hung, R. C. Myers, and M. Smolkin, JHEP 1410 (2014) 178;
H. Schnitzer, arXiv:1406.1161;
C. A. Agon, I. Cohen-Abbo, and H. J. Schnitzer, arxiv:1505.03757.

[54] D. Mumford, *Tata lectures on Theta III*, Progress in Mathematics **97**, Birkhäuser, Boston 1991;
J. Igusa, *Theta Functions*, Springer-Verlag (1972).

[55] J. Fay, *Theta functions on Riemann surfaces*, Lecture Notes in Mathematics **352**, Springer-Verlag, 1973.

[56] L. J. Dixon, D. Friedan, E. J. Martinec and S. H. Shenker, Nucl. Phys. B **282**, 13 (1987);
Al. B. Zamolodchikov, Nucl. Phys. B **285**, 481 (1987);
L. Alvarez-Gaumé, G. W. Moore, and C. Vafa, Commun. Math. Phys. **106**, 1 (1986);
E. Verlinde and H. Verlinde, Nucl. Phys. B **288**, 357 (1987);
V. G. Knizhnik, Commun. Math. Phys. **112**, 567 (1987);
M. Bershadsky and A. Radul, Int. J. Mod. Phys. A **2**, 165 (1987).

[57] R. Dijkgraaf, E. P. Verlinde, and H. L. Verlinde, Commun. Math. Phys. **115**, 649 (1988).

[58] P. Ginsparg, *Applied Conformal Field theory*, Les Houches lecture notes (1988), arXiv:hep-th/9108028.

[59] A. Coser, E. Tonni, and P. Calabrese, arXiv:1503.09114.

[60] M. Fagotti and P. Calabrese, J. Stat. Mech. P04016 (2010).

[61] K. Audenaert, J. Eisert, M. B. Plenio, and R. F. Werner, Phys. Rev. A **66**, 042327 (2002).

[62] A. Botero and B. Reznik, Phys. Rev. A **70**, 052329 (2004).

[63] I. Peschel and V. Eisler, J. Phys. A **42**, 504003 (2009).

[64] S. Marcovitch, A. Retzker, M. B. Plenio and B. Reznik, Phys. Rev. A **80**, 012325 (2009).

[65] J. Cardy and P. Calabrese, J. Stat. Mech. P04023 (2010).

[66] P. Calabrese, M. Campostrini, F. Essler and B. Nienhius, Phys. Rev. Lett **104**, 095701 (2010).

[67] P. Calabrese and F. H. L. Essler, J. Stat. Mech. P08029 (2010).

[68] J. C. Xavier and F. C. Alcaraz, Phys. Rev. B **83**, 214425 (2011);
    M. Fagotti and P. Calabrese, J. Stat. Mech. P01017 (2011);
    M. Dalmonte, E. Ercolessi, L. Taddia, Phys. Rev. B **84**, 085110 (2011);
    M. Dalmonte, E. Ercolessi, L. Taddia, Phys. Rev. B **85**, 165112 (2012);
    P. Calabrese, M. Mintchev, and E. Vicari, J. Stat. Mech. P09028 (2011).

[69] P. Facchi, G. Florio, C. Invernizzi and S. Pascazio, Phys. Rev. A **78**, 052302 (2008).

[70] A. Coser, E. Tonni, P. Calabrese, in preparation.

[71] V. Enolski and T. Grava, Int. Math. Res. Not. **32**, (2004) 1619.

[72] A. Erderlyi, *Higher transcendental functions*, vol. I, Mc Graw Hill, (1953).

[73] B. Derrida, M. Mendèz France, and J. Peyrière, J. Stat. Phys. **45**, 439 (1986).